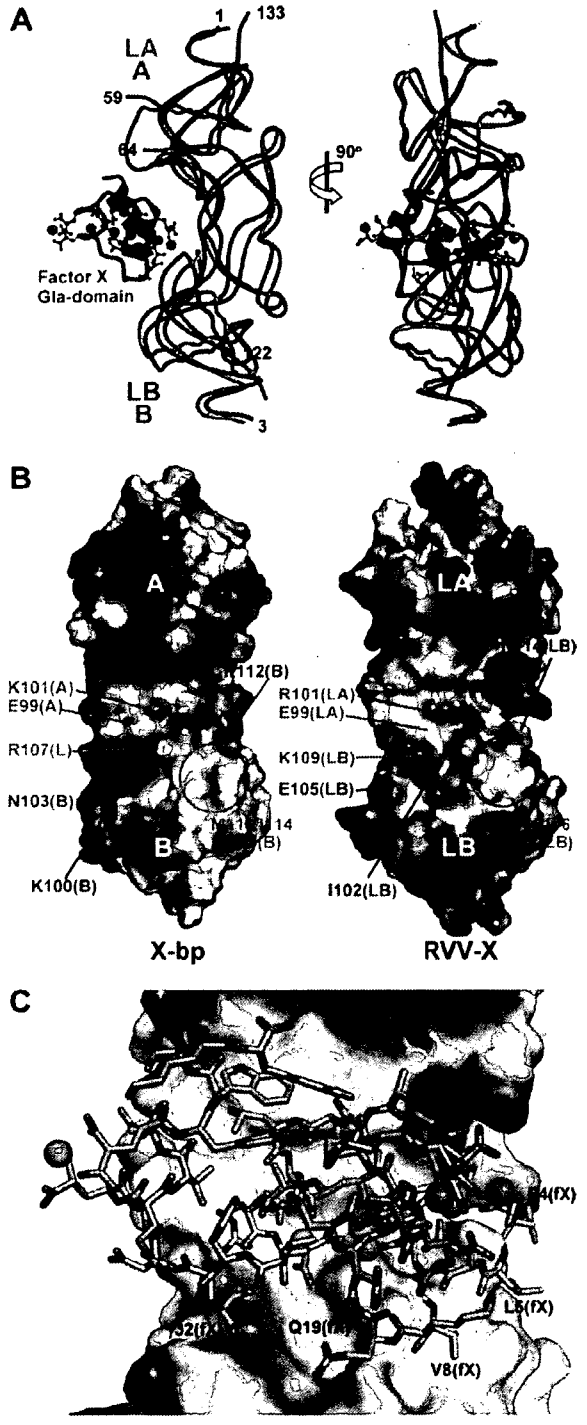

Fig. 2. Comparison of the RVV-X light chains and X-bp. (A) Superimposition of the RVV-X light chains (LA in orange and LB in magenta) onto the structure of X-bp (in gray) in complex with the Gla domain (in pink) of factor Xa (1IOD). The Gla residues and the Ca^{2+} ions are shown in ball-and-stick representation and as green spheres, respectively. (B) The molecular surfaces of X-bp and the light chains of RVV-X are represented according their electrochemical potentials (blue for positive, red for negative) and are viewed from the pseudo 2-fold axis. Conserved and varied residues are labelled in cyan and in red, respectively. (C) A model of the RVV-X light chains in complex with the Gla domain that was positioned based on the X-bp/fX Gla domain complex structure.

3.4. Docking model

Fig. 3A represents a preliminary docking model. For constructing a model, firstly, the second EGF domain (EGF2) and the serine proteinase (SP) domain of factor Xa (PDBID:1XKA) were placed such that the N-terminus of the factor X heavy chain (Ile195) closely approaches the RVV-X active site, and the globular SP domain fits into the concave

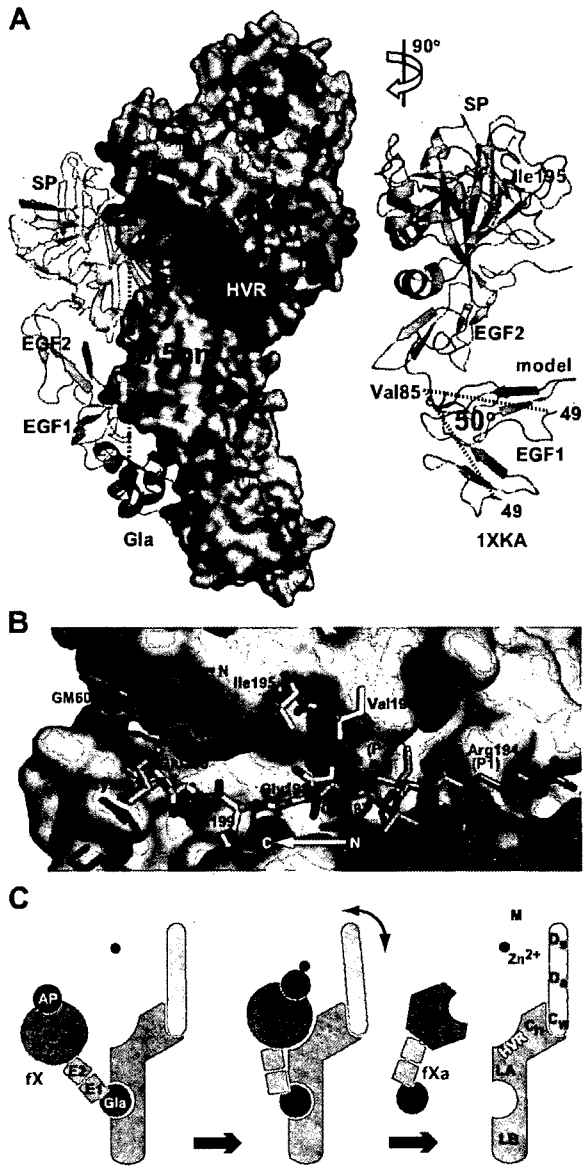

Fig. 3. Docking model. (A) The surfaces of the RVV-X sub-domains are coloured as in Fig. 1A. Factor Xa is shown in ribbon representation. Ile195 (in stick representation) and the N-terminal region (residues 195-201) of the factor X heavy chain are shown in magenta. In the right panel, the EGF1 segment of the original structural model (1XKA) is shown in gray. (B) Close up view of the RVV-X catalytic site of the docking model viewed from inside the factor Xa molecule. The N-terminal residues of factor Xa are shown in white and those of the model of factor X (zymogen) are shown in light pink. Because the factor X structure is currently unavailable, we assumed that this region has an extended structure. (C) Schematic model of factor X activation by RVV-X.

surface created by the C_h/LA domains. Secondly, we introduced a 50° bend between the two EGF domains so that the EGF1 domain fits to the convex surface of the LA domain (Fig. 3A). The linker between the two EGF domains is most likely flexible in solution [20]. This displacement successfully placed the N-terminus of the EGF1 domain in close proximity to the C-terminus of the Gla domain.

In the factor Xa structure, the N-terminal residue of the heavy chain, Ile195, is buried within the protein [20]. However, in the zymogen, the intact Arg194-Ile195-containing segment must be situated on the molecular surface, as in the equivalent segments of other serine proteinase zymogen structures [21]. The region of factor X that is C-terminal to the scissile peptide (segment coloured in magenta in Fig. 3A) may be located along the surface of the SP domain, resulting in its binding to the primed region of RVV-X, in the same orientation as the peptide-like inhibitor GM6001 lies in the current crystal structure (Fig. 3B). In the present docking model, since both molecules were positioned just as a rigid body without any collision, the active site zinc atom of RVV-X and Ile195 of factor Xa are 16 Å apart. Intrinsic hinge motions of the modular M/D_s/D_a/C_w architecture [12], and conformational changes upon association of RVV-X and the factor X zymogen, may allow the catalytic site of RVV-X to interact directly with the Arg194-Ile195 bond of factor X when in solution (Fig. 3C). The relatively large separation (~65 Å) of the catalytic site and the Gla-domain-binding exosite may explain the high specificity of RVV-X for factor X.

3.5. Implication for molecular evolution of RVV-X

CLPs from snake venoms are characterized by a unique dimerization mechanism of protein evolution, in which two monomers swap a portion of the long loop region, forming a stable functional unit and creating a new concave surface for target binding for a variety of biological activities [10]. Dimers can further aggregate with each other to form higher-order oligomers [22], or, as in the case of RVV-X, form covalently linked complexes with a metalloproteinase chain creating an exosite. The RVV-X structure illustrates a good example of evolutionary gain of function by multi-subunit proteins, represented by the fold adaptation, for the binding of other ligands.

4. Conclusion

ADAMs are widely distributed and constitute the major membrane-bound sheddases to play roles in important processes occurring at the cell surface. However, the molecular mechanism of target recognition by ADAMs and which ADAMs shed which key substrates in specific biological events has been poorly understood. Previously, we suggested that the HVR may constitute an exosite that captures the target or associated proteins, and that is processed by the catalytic site [11]. The RVV-X structure is consistent with this model and provides insights into the molecular basis of HVR-mediated protein–protein interactions and target recognition by ADAM/adamalysin/reprolysin family proteins.

Acknowledgements: The authors thank M. Tomisako for help in crystallization experiments, M. Kawamoto and N. Shimizu for assistance with data acquisition at the SPring-8 beamline BL41XU and T. Morita for helpful discussions. This work was partly supported by the Ministry of Education, Science, Sports and Culture, Grant-in-aid for Scientific Research B-19370047-2007, and Health and Labor Science Research Grants, and by grants from the Mitsubishi Pharma Research Foundation and the Astellas Foundation for Research on Metabolic Disorders. T.I is supported by the grant from New Energy and Industrial Technology Development Organization (NEDO) of Japan.

Appendix A. Supplementary data

The atomic coordinates and structure factors have been deposited in the NCBI protein data bank with the accession code 2E3X. Supplementary data associated with this article can be found, in the online version, at doi:10.1016/j.febslet.2007.11.062.

References

[1] Mann, K.G., Nesheim, M.E., Church, W.R., Haley, P. and Krishnaswamy, S. (1990) Surface-dependent reactions of the vitamin K-dependent enzyme complexes. Blood 76, 1–16.
[2] Morita, T. (1998) Proteases which activate factor X in: Enzymes from Snake Venom (Bailey, G.S., Ed.), pp. 179–208, Alaken, Colorado.
[3] Tans, G. and Rosing, J. (2001) Snake venom activators of factor X: an overview. Haemostasis 31, 225–233.
[4] Fox, J.W. and Serrano, S.M. (2005) Structural considerations of the snake venom metalloproteinases, key members of the M12 reprolysin family of metalloproteinases. Toxicon 45, 969–985.
[5] Gowda, D.C., Jackson, C.M., Hensley, P. and Davidson, E.A. (1994) Factor X-activating glycoprotein of Russell's viper venom. Polypeptide composition and characterization of the carbohydrate moieties. J. Biol. Chem. 269, 10644–10650.
[6] Kisiel, W., Hermodson, M.A. and Davie, E.W. (1976) Factor X activating enzyme from Russell's viper venom: isolation and characterization. Biochemistry 15, 4901–4906.
[7] Takeya, H., Nishida, S., Miyata, T., Kawada, S., Saisaka, Y., Morita, T. and Iwanaga, S. (1992) Coagulation factor X activating enzyme from Russell's viper venom (RVV-X). A novel metalloproteinase with disintegrin (platelet aggregation inhibitor)-like and C-type lectin-like domains. J. Biol. Chem. 267, 14109–14117.
[8] White, J.M. (2003) ADAMs: modulators of cell–cell and cell–matrix interactions. Curr. Opin. Cell Biol. 15, 598–606.
[9] Seals, D.F. and Courtneidge, S.A. (2003) The ADAMs family of metalloproteases: multidomain proteins with multiple functions. Genes Dev. 17, 7–30.
[10] Morita, T. (2005) Structures and functions of snake venom CLPs (C-type lectin-like proteins) with anticoagulant-, procoagulant-, and platelet-modulating activities. Toxicon 45, 1099–1114.
[11] Takeda, S., Igarashi, T., Mori, H. and Araki, S. (2006) Crystal structures of VAP1 reveal ADAMs' MDC domain architecture and its unique C-shaped scaffold. EMBO J. 25, 2388–2396.
[12] Igarashi, T., Araki, S., Mori, H. and Takeda, S. (2007) Crystal structures of catrocollastatin/VAP2B reveal a dynamic, modular architecture of ADAM/adamalysin/reprolysin family proteins. FEBS Lett. 581, 2416–2422.
[13] Gomis-Ruth, F.X. (2003) Structural aspects of the metzincin clan of metalloendopeptidases. Mol. Biotechnol. 24, 157–202.
[14] Weis, W.I., Kahn, R., Fourme, R., Drickamer, K. and Hendrickson, W.A. (1991) Structure of the calcium-dependent lectin domain from a rat mannose-binding protein determined by MAD phasing. Science 254, 1608–1615.
[15] Mizuno, H., Fujimoto, Z., Atoda, H. and Morita, T. (2001) Crystal structure of an anticoagulant protein in complex with the Gla domain of factor X. Proc. Natl. Acad. Sci. USA 98, 7230–7234.
[16] Atoda, H., Ishikawa, M., Mizuno, H. and Morita, T. (1998) Coagulation factor X-binding protein from Deinagkistrodon acutus venom is a Gla domain-binding protein. Biochemistry 37, 17361–17370.

[17] Lindhout, M.J., Kop-Klaassen, B.H. and Hemker, H.C. (1978) Activation of decarboxyfactor X by a protein from Russell's viper venom. Purification and partial characterization of activated decarboxyfactor X. Biochim. Biophys. Acta 533, 327–341.
[18] Morita, T. and Jackson, C.M. (1986) Preparation and properties of derivatives of bovine factor X and factor Xa from which the gamma-carboxyglutamic acid containing domain has been removed. J. Biol. Chem. 261, 4015–4023.
[19] Skogen, W.F., Bushong, D.S., Johnson, A.E. and Cox, A.C. (1983) The role of the Gla domain in the activation of bovine coagulation factor X by the snake venom protein XCP. Biochem. Biophys. Res. Commun. 111, 14–20.
[20] Kamata, K., Kawamoto, H., Honma, T., Iwama, T. and Kim, S.H. (1998) Structural basis for chemical inhibition of human blood coagulation factor Xa. Proc. Natl. Acad. Sci. USA 95, 6630–6635.
[21] Freer, S.T., Kraut, J., Robertus, J.D., Wright, H.T. and Xuong, N.H. (1970) Chymotrypsinogen: 2.5-angstrom crystal structure, comparison with alpha-chymotrypsin, and implications for zymogen activation. Biochemistry 9, 1997–2009.
[22] Fukuda, K., Mizuno, H., Atoda, H. and Morita, T. (2000) Crystal structure of flavocetin-A, a platelet glycoprotein Ib-binding protein, reveals a novel cyclic tetramer of C-type lectin-like heterodimers. Biochemistry 39, 1915–1923.

Journal of the American College of Cardiology
© 2007 by the American College of Cardiology Foundation
Published by Elsevier Inc.

Vol. 50, No. 13, 2007
ISSN 0735-1097/07/$32.00
doi:10.1016/j.jacc.2007.05.039

PRECLINICAL STUDIES

Important Role of Endogenous Hydrogen Peroxide in Pacing-Induced Metabolic Coronary Vasodilation in Dogs In Vivo

Toyotaka Yada, MD, PHD,* Hiroaki Shimokawa, MD, PHD,† Osamu Hiramatsu, PHD,* Yoshiro Shinozaki, BS,‡ Hidezo Mori, MD, PHD,§ Masami Goto, MD, PHD,* Yasuo Ogasawara, PHD,* Fumihiko Kajiya, MD, PHD*

Kurashiki, Sendai, Isehara, and Suita, Japan

Objectives We examined whether endogenous hydrogen peroxide (H_2O_2) is involved in pacing-induced metabolic vasodilation in vivo.

Background We have previously demonstrated that endothelium-derived H_2O_2 is an endothelium-derived hyperpolarizing factor in canine coronary microcirculation in vivo. However, the role of endogenous H_2O_2 in metabolic coronary vasodilation in vivo remains to be examined.

Methods Canine subepicardial small coronary arteries (≥100 μm) and arterioles (<100 μm) were continuously observed by a microscope under cyclooxygenase blockade (ibuprofen, 12.5 mg/kg intravenous [IV]) (n = 60). Experiments were performed during paired right ventricular pacing under the following 7 conditions: control, nitric oxide (NO) synthase inhibitor (N^G-monomethyl-L-arginine [L-NMMA], 2 μmol/min for 20 min intracoronary [IC]), catalase (a decomposer of H_2O_2, 40,000 U/kg IV and 240,000 U/kg/min for 10 min IC), 8-sulfophenyltheophylline (SPT) (an adenosine receptor blocker, 25 μg/kg/min for 5 min IC), L-NMMA+catalase, L-NMMA+tetraethylammonium (TEA) (K_{Ca}-channel blocker, 10 μg/kg/min for 10 min IC), and L-NMMA+catalase+8-SPT.

Results Cardiac tachypacing (60 to 120 beats/min) caused coronary vasodilation in both-sized arteries under control conditions in response to the increase in myocardial oxygen consumption. The metabolic coronary vasodilation was decreased after L-NMMA in subepicardial small arteries with an increased fluorescent H_2O_2 production compared with catalase group, whereas catalase decreased the vasodilation of arterioles with an increased fluorescent NO production compared with the L-NMMA group, and 8-SPT also decreased the vasodilation of arterioles. Furthermore, the metabolic coronary vasodilation was markedly attenuated after L-NMMA+catalase, L-NMMA+TEA, and L-NMMA+catalase+8-SPT in both-sized arteries.

Conclusions These results indicate that endogenous H_2O_2 plays an important role in pacing-induced metabolic coronary vasodilation in vivo. (J Am Coll Cardiol 2007;50:1272–8) © 2007 by the American College of Cardiology Foundation

Cardiac tachycardia by pacing or exercise increases myocardial oxygen consumption (MVO_2) and increases coronary blood flow by several mechanisms (1–3). Shear stress plays a crucial role in modulating vascular tone by endothelium-derived releasing factors (EDRFs), including nitric oxide (NO), prostacyclin (PGI_2), and endothelium-derived hyperpolarizing factor (EDHF) (4,5). Flow-induced vasodilation is mediated by either NO (6,7), PGI_2 (8), both of them (9), or EDHF (10). Matoba et al. have previously identified that endothelium-derived hydrogen peroxide (H_2O_2) is a primary EDHF in mesenteric arteries of mice and humans (11,12). Morikawa et al. (13,14) subsequently confirmed

See page 1279

From the *Department of Medical Engineering and Systems Cardiology, Kawasaki Medical School, Kurashiki, Japan; †Department of Cardiovascular Medicine, Tohoku University Graduate School of Medicine, Sendai, Japan; ‡Department of Physiology, Tokai University School of Medicine, Isehara, Japan; and the §Department of Cardiac Physiology, National Cardiovascular Center Research Institute, Suita, Japan. Dr. Yada is the winner of the Endothelium-Derived Hyperpolarizing Factor (EDHF) Tanabe Award from the Scientific Sessions of the American Heart Association, November 2005, Dallas, Texas.

This work was supported in part by grants from the Japanese Ministry of Education, Science, Sports, Culture, and Technology, Tokyo, Japan, Nos. 16209027 (to Dr. Shimokawa) and 16300164 (to Dr. Yada), the Program for Promotion of Fundamental Studies in Health Sciences of the Organization for Pharmaceutical Safety and Research of Japan (to Dr. Shimokawa), and Takeda Science Foundation 2002 (to Dr. Yada).

Manuscript received September 11, 2006; revised manuscript received April 25, 2007, accepted May 1, 2007.

that endothelial Cu,Zn-superoxide dismutase (SOD) plays an important role as an EDHF synthase in mice and humans. Miura et al. (15) demonstrated that endothelium-derived H_2O_2 is involved as an EDHF in the flow-induced vasodilation of isolated human coronary arterioles in vitro. We have recently confirmed that endogenous H_2O_2 plays an important compensatory role during coronary autoregulation (16) and reperfusion injury in vivo (17) through the interactions with NO and adenosine.

It is known that vascular α-adrenergic receptor is modulated by the endothelium in dogs (18), whereas cardiac β-adrenergic receptor is modulated by K_{Ca} channels in pigs (19) and H_2O_2 in mice (20). However, the role of endogenous H_2O_2 in metabolic coronary vasodilation in vivo remains largely unknown. In the present study, we thus examined whether H_2O_2 is involved in pacing-induced metabolic coronary vasodilation in canine coronary microcirculation in vivo.

Methods

This study conformed to the Guideline on Animal Experiments of Kawasaki Medical School and the Guide for the Care and Use of Laboratory Animals published by the U.S. National Institutes of Health.

Animal preparation. Anesthetized mongrel dogs of either gender (15 to 25 kg in body weight, n = 60) were ventilated with a ventilator (Model VS600, IDC, Pittsburgh, Pennsylvania). We continuously monitored aortic pressure and left ventricular pressure (LVP) with a catheter (SPC-784A, Millar, Houston, Texas) and blood flow of the left anterior descending coronary artery (LAD) with a transonic flow probe (T206, Transonic Systems, Ithaca, New York).

Measurements of coronary diameter by intravital microscope. We continuously monitored coronary vascular responses by an intravital microscope (VMS 1210, Nihon Kohden, Tokyo, Japan) with a needle-probe in vivo, as previously described (21). We gently placed the needle-probe on subepicardial microvessels. When a clear vascular image was obtained, end-diastolic vascular images were taken with 30 pictures/s (21).

Measurements of regional myocardial blood flow. Regional myocardial blood flow was measured by the nonradioactive microsphere (Sekisui Plastic Co. Ltd., Tokyo, Japan) technique, as previously described (22). Briefly, the microspheres suspension was injected into the left atrium 3 min after tachypacing. Myocardial flow in the LAD area was calculated according to the formula "time flow = tissue counts × (reference flow/reference counts)" and was expressed in ml/g/min (22).

Detection of H_2O_2 and NO production in coronary microvessels. 2′,7′-dichlorodihydrofluorescein diacetate (DCF) (Molecular Probes, Eugene, Oregon) and diaminorhodamine-4M AM (DAR) (Daiichi Pure Chemicals, Tokyo, Japan) were used to detect H_2O_2 and NO production in coronary microvessels, respectively, as previously described (17). Briefly, fresh and unfixed heart tissues were cut into several blocks and immediately frozen in optimal cutting temperature compound (Tissue-Tek, Sakura Fine Chemical, Tokyo, Japan). Fluorescent images of the microvessels were obtained 3 min after application of acetylcholine (ACh) by using a fluorescence microscope (OLYMPUS BX51, Tokyo, Japan) (17).

Experimental protocols. After the surgical procedure and instrumentation, at least 30 min were allowed for stabilization while monitoring hemodynamic variables. Coronary vasodilator responses were examined before and after cardiac tachypacing (60 to 120 beats/min) under the following 7 conditions with cyclooxygenase blockade (ibuprofen, 12.5 mg/kg, IV) to evaluate the role of H_2O_2 and NO without PGI_2 in a different set of animals (Fig. 1): 1) control conditions without any inhibitor; 2) L-NMMA alone (2 μmol/min intracoronary [IC] for 20 min); 3) catalase alone (40,000 U/kg intravenous [IV] and 240,000 U/kg/min IC for 10 min, an enzyme that dismutates

Abbreviations and Acronyms

CBF = coronary blood flow
DAR = diaminorhodamine-4M AM
DCF = 2′,7′-dichlorodihydrofluorescein diacetate
EDHF = endothelium-derived hyperpolarizing factor
H_2O_2 = hydrogen peroxide
L-NMMA = N^G-monomethyl-L-arginine
LAD = left anterior descending coronary artery
MVO_2 = myocardial oxygen consumption
NO = nitric oxide
PGI_2 = prostacyclin
SPT = sulfophenyltheophylline
TEA = tetraethylammonium

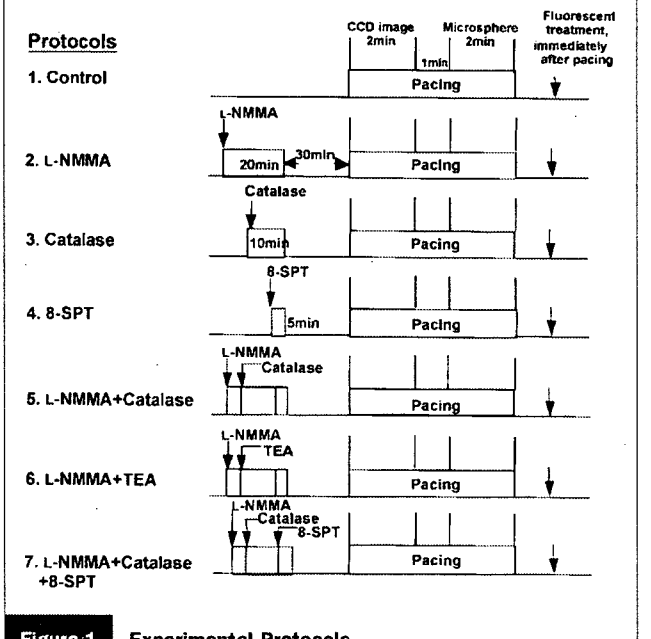

Figure 1 Experimental Protocols

CCD = charge-coupled device; L-NMMA = N^G-monomethyl-L-arginine; SPT = sulfophenyltheophylline; TEA = tetraethylammonium.

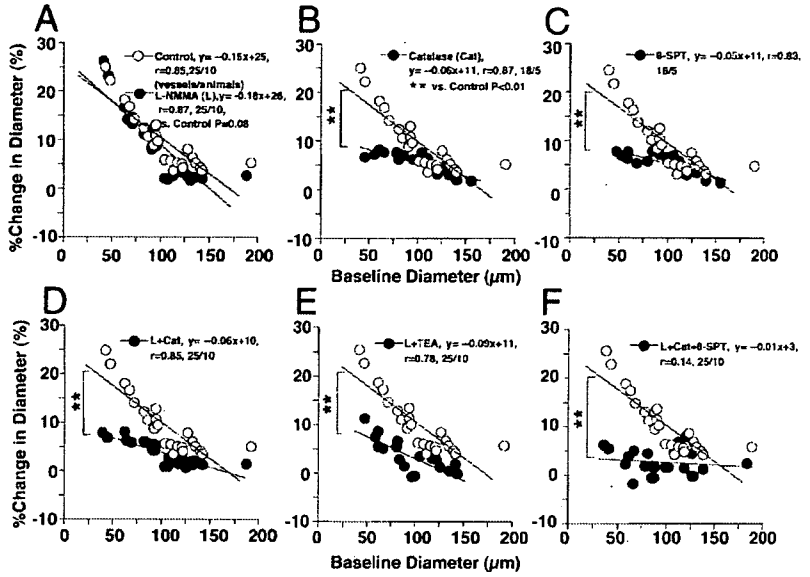

Figure 2 **Coronary Vascular Responses to Cardiac Pacing**

The coronary vasodilating responses of both-sized coronary arteries were significantly inhibited in all experimental conditions except L-NMMA alone. **p < 0.01. Abbreviations as in Figure 1.

H_2O_2 into water and oxygen); 4) adenosine receptor blockade alone (8-sulfophenyltheophylline [8-SPT], 25 μg/kg/min IC for 5 min); 5) catalase plus L-NMMA; 6) catalase plus tetraethylammonium (TEA) (10 μg/kg/min IC for 10 min, an inhibitor of large conductance K_{Ca} channels to inhibit EDHF-mediated responses) (23); and 7) catalase plus L-NMMA with 8-SPT (16). These inhibitors were given at 30 min before cardiac tachypacing (Fig. 1). The basal coronary diameter was defined as that before pacing. We continuously observed the diameter change in subepicardial small coronary arteries (≥100 μm) and arterioles (<100 μm) with an intravital microscope before and at 2 min after pacing. Microspheres were administered at 3 min after the pacing was started (Fig. 1). In the combined infusion protocol (L-NMMA+catalase+8-SPT), L-NMMA infusion was first started, followed by catalase infusion, and then 8-SPT was added at 15 min after the initiation of L-NMMA infusion (Fig. 1). Then, fresh and unfixed heart tissues were cut into several blocks and immediately frozen in optimal cutting temperature compound after the pacing. The flow and MVO_2 were measured as full-thickness values.

Drugs. All drugs were obtained from Sigma Chemical Co. and were diluted in a physiological saline immediately before use.

Statistical analysis. Results are expressed as means ± SEM. Differences in the vasodilation of subepicardial coronary microvessels before and after pacing (Fig. 2) were examined by a multiple regression analysis using a model, in which the change in coronary diameter was set as a dependent variable (y) and vascular size as an explanatory variable (x), while the statuses of control and other inhibitors were set as dummy variables (D1, D2) in the following equation: $y = a0 + a1x + a2D1 + a3D2$, where a0 through a3 are partial regression coefficients (16). Significance tests were made as simultaneous tests for slope and intercept differences. Pairwise comparisons against control were made without adjustment for multiple comparisons. The vessel was the unit of analysis without correction for correlated observations. The power of this analysis is greater than that of using the animal as the unit of analysis, giving smaller p values. Vascular fluorescent responses (Figs. 3 and 4) were analyzed by one-way analysis of variance followed by Scheffe's post hoc test for multiple comparisons. The criterion for statistical significance was at $p < 0.05$.

Results

Hemodynamic status and blood gases during pacing. Throughout the experiments, mean aortic pressure was constant and comparable (Table 1), and pO_2, pCO_2, and pH were maintained within the physiological ranges (pO_2 >70 mm Hg, pCO_2 25 to 40 mm Hg, and pH 7.35 to 7.45). Baseline coronary diameter was comparable in the absence and presence of inhibitors under the 7 different experimental conditions (Table 1). Cardiac tachypacing increased coronary blood flow and MVO_2 from the baseline values (Table 2, both $p < 0.01$). Combined infusion of L-NMMA+catalase+8-SPT significantly decreased coronary blood flow (CBF) and MVO_2 as compared with control, L-NMMA alone (both $p < 0.01$), catalase alone (both $p < 0.01$), 8-SPT alone (both $p < 0.01$), L-NMMA+catalase (both $p < 0.05$), L-NMMA+TEA (both $p < 0.05$). Com-

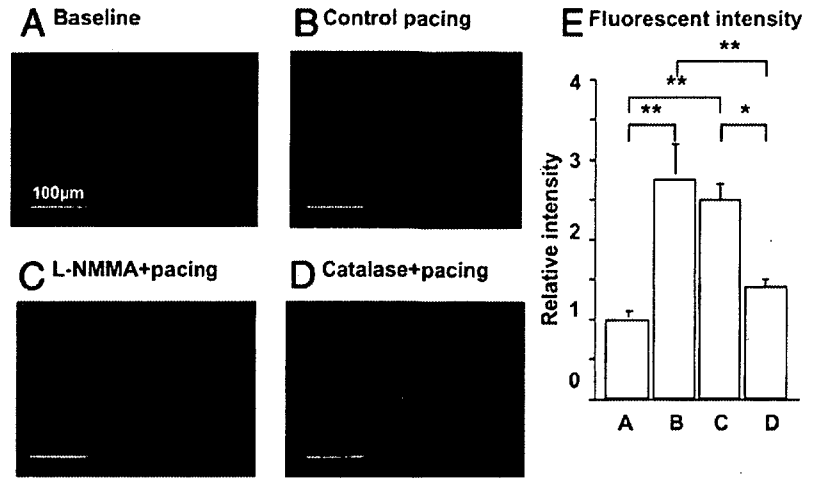

Figure 3 **Detection of H_2O_2 Production With DCF Fluorescent Method**

Hydrogen peroxide (H_2O_2) production was unaltered after N^G-monomethyl-L-arginine (L-NMMA) but was markedly suppressed by catalase. Number of arterioles/animals used was 5/5 for each group. *p < 0.05, **p < 0.01. DCF = 2',7'-dichlorodihydrofluorescein diacetate.

bined infusion of L-NMMA+catalase or L-NMMA+TEA significantly decreased CBF (both $p < 0.05$) and MVO_2 (both $p < 0.05$) as compared with control after the pacing.

Coronary vasodilation before and after cardiac tachypacing. Cardiac tachypacing caused coronary vasodilation in both-sized arteries under control conditions (small coronary arteries, 5 ± 1%; arterioles, 14 ± 2%) (Fig. 2A) with decreased coronary venous pO_2 (Table 2). The metabolic coronary vasodilation was significantly decreased after L-NMMA in small coronary arteries (3 ± 1%) but not in arterioles (14 ± 2%), whereas catalase and 8-SPT decreased the vasodilation of arterioles (both 4 ± 1%) but not in small coronary arteries (both 7 ± 1%) (Figs. 2B and 2C). Furthermore, the metabolic coronary vasodilation was markedly attenuated after L-NMMA+catalase and L-NMMA+TEA in small coronary arteries (both 2 ± 1%), and L-NMMA+catalase+8-SPT almost abolished the vasodilating responses in both-sized arteries (small coronary arteries, −1 ± 1%; arterioles, 1 ± 1%) (Figs. 2D to 2F). When expressed in a linear regression analysis, the coronary vasodilating responses of both-sized coronary arteries were significantly inhibited in all experimental conditions except L-NMMA alone (Fig. 2A).

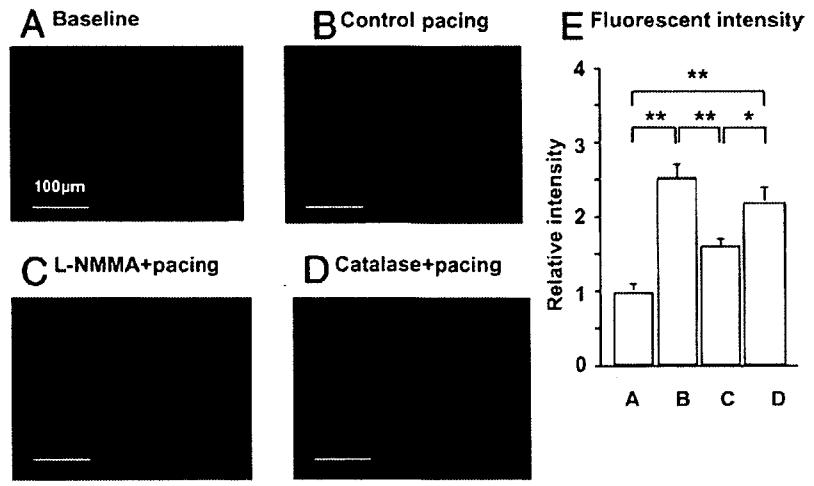

Figure 4 **Detection of NO Production With DAR Fluorescent Method**

Nitric oxide (NO) production was unaltered after catalase but was markedly suppressed by N^G-monomethyl-L-arginine (L-NMMA). Number of arterioles/animals used was 5/5 for each group. *p < 0.05, **p < 0.01. DAR = diaminorhodamine-4M AM.

JACC Vol. 50, No. 13, 2007
September 25, 2007:1272–8

Table 1 The Small Artery and Arteriolar Diameter Measurements at Rest and During Cardiac Pacing

	Control	L-NMMA (L)	Catalase (Cat)	8-SPT	L+Cat	L+TEA	L+Cat+8-SPT
Small artery							
n (vessels/dogs)	12/10	12/10	9/5	7/5	12/10	12/10	12/10
Rest (μm)	127 ± 7	125 ± 6	127 ± 5	126 ± 6	125 ± 7	123 ± 6	124 ± 7
Cardiac pacing (μm)	134 ± 7*	129 ± 7†	132 ± 5*	131 ± 6*	127 ± 7	124 ± 6	123 ± 6
Arteriole							
n (vessels/dogs)	12/10	12/10	9/5	9/5	12/10	12/10	12/10
Rest (μm)	75 ± 5	73 ± 5	71 ± 5	71 ± 5	72 ± 5	74 ± 5	72 ± 6
Cardiac pacing (μm)	85 ± 5*	82 ± 5*	77 ± 6†	77 ± 6†	77 ± 5†	77 ± 5	73 ± 5

Results are expressed as mean ± SEM. *$p < 0.01$, †$p < 0.05$ versus rest.
L-NMMA = N^G-monomethyl-L-arginine; SPT = sulfophenyltheophylline; TEA = tetraethylammonium.

Detection of H_2O_2 and NO production. Fluorescent microscopy with DCF showed that cardiac tachypacing increased coronary H_2O_2 production compared with baseline conditions in arterioles (Fig. 3). The pacing-induced H_2O_2 production as assessed by DCF fluorescent intensity was unaltered after L-NMMA but was markedly suppressed by catalase (Fig. 3). By contrast, in small coronary arteries, vascular NO production as assessed by DAR fluorescent intensity was significantly increased in response to the pacing compared with baseline conditions (Fig. 4). The pacing-induced NO production was unaltered after catalase but was markedly suppressed by L-NMMA (Fig. 4). Pacing caused no significant increase in H_2O_2 production in small coronary arteries or NO production in arterioles (data not shown).

Discussion

The major finding of the present study is that endogenous H_2O_2 plays an important role in pacing-induced metabolic coronary dilation as a compensatory mechanism for NO in vivo. We demonstrated the important role of endogenous H_2O_2 in the mechanisms for metabolic coronary dilation in vivo.

Validations of experimental model and methodology. We chose, on the basis of our previous reports (16,17), the adequate dose of L-NMMA, catalase, TEA, and 8-SPT in order to inhibit NO synthesis, H_2O_2, K_{Ca} channels, and the adenosine receptor, respectively. The TEA at low doses is fairly specific for K_{Ca} channel, but at higher doses it might block a number of other K channels. Because several K_{Ca} channels might be involved in H_2O_2-mediated responses (5), we selected nonselective K_{Ca} inhibitor, TEA, to inhibit all K_{Ca} channels (23). We have previously confirmed the validity of our present methods (21).

Role of NO and H_2O_2 after cardiac pacing. Matoba et al. have demonstrated that endothelium-derived H_2O_2 is an EDHF in mouse (11) and human (12) mesenteric arteries and pig coronary microvessels (24). Morikawa et al. also

Table 2 Hemodynamic Status at Rest and During Cardiac Pacing

	Control	L-NMMA (L)	Catalase (Cat)	8-SPT	L+Cat	L+TEA	L+Cat+8-SPT
n (dogs)	10	10	5	5	10	10	10
SBP							
Rest (mm Hg)	135 ± 14	135 ± 14	114 ± 9	123 ± 5	98 ± 9	99 ± 9	96 ± 8
Cardiac pacing	137 ± 14	136 ± 14	125 ± 12	130 ± 7	100 ± 9	100 ± 8	103 ± 9
MBP							
Rest (mm Hg)	117 ± 10	117 ± 10	98 ± 8	99 ± 5	89 ± 10	90 ± 10	87 ± 9
Cardiac pacing	124 ± 9	120 ± 13	107 ± 10	110 ± 7	91 ± 10	92 ± 10	92 ± 10
DP							
Rest	8,100 ± 845	8,100 ± 845	6,855 ± 527	7,350 ± 312	5,880 ± 537	5,910 ± 527	5,730 ± 478
Cardiac pacing	16,440 ± 1,718*	16,320 ± 1,680*	15,000 ± 1,423*	15,630 ± 778*	11,940 ± 11,029*	12,000 ± 1,011*	12,300 ± 1,078*
$CVPO_2$							
Rest (mm Hg)	20 ± 1	17 ± 1	16 ± 1	17 ± 1	15 ± 1†	15 ± 1†	14 ± 1†
Cardiac pacing	14 ± 1*	11 ± 1*	11 ± 1*	12 ± 1*	10 ± 1*†	10 ± 1*†	9 ± 1*†
MVO_2							
Rest (μlO_2/min/g)	70 ± 2	66 ± 2	67 ± 2	73 ± 5	62 ± 5	61 ± 5	60 ± 5
Cardiac pacing	171 ± 4‡	168 ± 2‡	158 ± 12‡	168 ± 13‡	133 ± 4†‡	130 ± 18†‡	95 ± 9*§
CBF							
Rest (ml/min/g)	0.66 ± 0.06	0.63 ± 0.06	0.66 ± 0.03	0.66 ± 0.01	0.59 ± 0.06	0.62 ± 0.05	0.51 ± 0.04
Cardiac pacing	1.48 ± 0.32‡	1.46 ± 0.06‡	1.36 ± 0.02‡	1.40 ± 0.01‡	1.22 ± 0.01†‡	1.24 ± 0.12†‡	0.96 ± 0.07‡§

Results are expressed as mean ± SEM. *$p < 0.05$ versus at rest. †$p < 0.05$ versus corresponding control measurements. ‡$p < 0.01$ versus rest. §$p < 0.01$ versus corresponding control measurements.
CBF = coronary blood flow; $CVPO_2$ = coronary venous pO_2; DP = double product; MBP = mean blood pressure; MVO_2 = myocardial oxygen consumption; SBP = systolic blood pressure; other abbreviations as in Table 2.

have demonstrated that endothelial Cu,Zn-SOD plays an important role as an H_2O_2/EDHF synthase in mouse (13) and human (14) mesenteric arteries. Subsequently, we (16,17) and others (15) confirmed that endogenous H_2O_2 exerts important vasodilator effects in canine coronary microcirculation in vivo and in isolated human coronary microvessels, respectively. In the present study, the pacing-induced metabolic coronary vasodilation was significantly decreased after L-NMMA in small coronary arteries but not in arterioles, whereas catalase decreased the vasodilation of arterioles but not that of small arteries, and the coronary vasodilation was markedly attenuated after L-NMMA+catalase (Fig. 2). These findings indicate that NO and H_2O_2 compensate for each other to maintain coronary vasodilation in response to increased myocardial oxygen demand. Coronary venous pO_2 tended to be lower after L-NMMA+catalase, suggesting that NO and H_2O_2 coordinately cause coronary vasodilation during cardiac tachypacing.

Saitoh et al. (25) suggested that the production of H_2O_2, which stems from the dismutation of $\cdot O_2^-$ that is formed during mitochondrial electron transport, is seminal in the coupling between oxygen metabolism and blood flow in the heart. Thus, the contribution of H_2O_2 production in response to the change in metabolism cannot be excluded.

Endothelial Cu,Zn-SOD plays an important role in the synthesis of H_2O_2 as an EDHF synthase in mouse (13) and human (14) mesenteric arteries, and exercise training enhances expression of Cu,Zn-SOD in normal pigs (26). It remains to be examined whether exercise-induced upregulation of Cu,Zn-SOD enhances metabolic coronary vasodilation mediated by endogenous H_2O_2.

Compensatory vasodilator mechanism among H_2O_2, NO, and adenosine. The EDHF acts as a partial compensatory mechanism to maintain endothelium-dependent vasodilation in the forearm microcirculation of patients with essential hypertension, where NO activity is impaired owing to oxidative stress (27). We have recently demonstrated in the fluorescent microscopy study that coronary vascular production of H_2O_2 and NO is enhanced after myocardial ischemia/reperfusion in small coronary arteries and arterioles, respectively (17). In the present study, the DCF fluorescent intensity was comparable between control and L-NMMA, and that of DAR was also comparable between control and catalase (Figs. 3 and 4). Although the exact source of vascular production of H_2O_2 and NO remains to be elucidated, it is highly possible that endothelium-derived NO and H_2O_2 compensate for each other to maintain coronary vasodilation in response to increased MVO_2.

In the dog, blockade of any vasodilator mechanisms fails to blunt the increase in coronary blood flow in response to exercise, indicating that adenosine, K^+_{ATP}-channel opening, prostanoids, or NO might not be mandatory for exercise-induced coronary vasodilation, or that these redundant vasodilator mechanisms compensate for each other when one mechanism is blocked (28). In the present study, adenosine blockade with 8-SPT alone inhibited the pacing-induced vasodilation of arteriole but not that of small artery, whereas combined administration of L-NMMA+catalase+8-SPT almost abolished the pacing-induced coronary vasodilation of both-sized arteries with an increase in coronary blood flow (Fig. 2). The discrepancy between the diameter and flow responses is likely due to the metabolic autoregulation of smaller arterioles. These results indicate that adenosine also plays an important role to maintain metabolic coronary vasodilation in cooperation with NO and H_2O_2, a finding consistent with our previous study on coronary autoregulatory mechanisms (15).

Study limitations. Several limitations should be mentioned for the present study. First, although we were able to demonstrate the production of H_2O_2 with fluorescent microscopy with DCF, we were unable to quantify the endothelial H_2O_2 production, because DCF reacts with H_2O_2, peroxynitrite, and hypochlorous acid (13). Second, we were unable to find smaller arterioles, owing to the limited spatial resolution of our charge-coupled device intravital microscope. With an intravital camera with higher resolution, we would be able to observe coronary vasodilation of smaller arterioles. Third, we were unable to determine whether H_2O_2 is produced by shear stress or cardiac metabolism. This point remains to be elucidated in a future study.

Conclusions

We were able to demonstrate that endogenous H_2O_2 plays an important role in pacing-induced metabolic coronary vasodilation in canine coronary microcirculation in vivo and that there are substantial compensatory interactions among NO, H_2O_2, and adenosine to maintain metabolic coronary vasodilation, which is one of the most important mechanisms for cardiovascular homeostasis in vivo.

Reprint requests and correspondence: Dr. Toyotaka Yada, Department of Medical Engineering and Systems Cardiology, Kawasaki Medical School, 577 Matsushima, Kurashiki, Okayama 701-0192, Japan. E-mail: yada@me.kawasaki-m.ac.jp.

REFERENCES

1. Ishibashi Y, Duncker DJ, Zhang J, Bache RJ. ATP-sensitive K^+ channels, adenosine, and nitric oxide-mediated mechanisms account for coronary vasodilation during exercise. Circ Res 1998;82:346–59.
2. Jones CJ, Kuo L, Davis MJ, DeFily DV, Chilian WM. Role of nitric oxide in the coronary microvascular responses to adenosine and increased metabolic demand. Circulation 1995;91:1807–13.
3. Yada T, Richmond KN, Van Bibber R, Kroll K, Feigl EO. Role of adenosine in local metabolic coronary vasodilation. Am J Physiol 1999;276:H1425–33.
4. Feletou M, Vanhoutte PM. Endothelium-dependent hyperpolarization of canine smooth muscle. Br J Pharmacol 1988;93:515–24.
5. Shimokawa H. Primary endothelial dysfunction: atherosclerosis. J Mol Cell Cardiol 1999;31:23–37.
6. Kuo L, Davis MJ, Chilian WM. Endothelium-dependent, flow-induced dilation of isolated coronary arterioles. Am J Physiol 1991; 259:H1063–70.

7. Kuo L, Chilian WM, Davis MJ. Interaction of pressure- and flow-induced responses in porcine coronary resistance vessels. Am J Physiol 1991;261:H1706–15.
8. Koller A, Sun D, Kaley G. Role of shear stress and endothelial prostaglandins in flow- and viscosity-induced dilation of arterioles in vitro. Circ Res 1993;72:1276–84.
9. Koller A, Sun D, Huang A, Kaley G. Corelease of nitric oxide and prostaglandins mediates flow-dependent dilation of ratgracilis muscle arterioles. Am J Physiol 1994;267:H326–32.
10. Takamura Y, Shimokawa H, Zhao H, et al. Important role of endothelium-derived hyperpolarizing factor in shear stress-induced endothelium-dependent relaxations in the rat mesenteric artery. J Cardiovasc Pharmacol 1999;34:381–7.
11. Matoba T, Shimokawa H, Nakashima M, et al. Hydrogen peroxide is an endothelium-derived hyperpolarizing factor in mice. J Clin Invest 2000;106:1521–30.
12. Matoba T, Shimokawa H, Kubota H, et al. Hydrogen peroxide is an endothelium-derived hyperpolarizing factor in human mesenteric arteries. Biochem Biophys Res Comm 2002;290:909–13.
13. Morikawa K, Shimokawa H, Matoba T, et al. Pivotal role of Cu,Zn-superoxide dismutase in endothelium-dependent hyperpolarization. J Clin Invest 2003;112:1871–9.
14. Morikawa K, Fujiki T, Matoba T, et al. Important role of superoxide dismutase in EDHF-mediated responses of human mesenteric arteries. J Cardiovasc Pharmacol 2004;44:552–6.
15. Miura H, Bosnjak JJ, Ning G, Saito T, Miura M, Gutterman DD. Role for hydrogen peroxide in flow-induced dilation of human coronary arterioles. Circ Res 2003;92:e31–40.
16. Yada T, Shimokawa H, Hiramatsu O, et al. Hydrogen peroxide, an endogenous endothelium-derived hyperpolarizing factor, plays an important role in coronary autoregulation in vivo. Circulation 2003; 107:1040–5.
17. Yada T, Shimokawa H, Hiramatsu O, et al. Cardioprotective role of endogenous hydrogen peroxide during ischemia-reperfusion injury in canine coronary microcirculation in vivo. Am J Physiol 2006;291: H1138–46.
18. Jones CJ, DeFily DV, Patterson JL, Chilian WM. Endothelium-dependent relaxation competes with alpha 1- and alpha 2-adrenergic constriction in the canine epicardial coronary microcirculation. Circulation 1993;87:1264–74.
19. Scornik FS, Codina J, Birnbaumer L, Toro L. Modulation of coronary smooth muscle K_{Ca} channels by Gs alpha independent of phosphorylation by protein kinase A. Am J Physiol 1993;265:H1460–5.
20. Tan CM, Xenoyannis S, Feldman RD. Oxidant stress enhances adenylyl cyclase activation. Circ Res 1995;77:710–7.
21. Yada T, Hiramatsu O, Kimura A, et al. In vivo observation of subendocardial microvessels of the beating porcine heart using a needle-probe videomicroscope with a CCD camera. Circ Res 1993; 72:939–46.
22. Mori H, Haruyama Y, Shinozaki H, et al. New nonradioactive microspheres and more sensitive X-ray fluorescence to measure regional blood flow. Am J Physiol 1992;263:H1946–57.
23. Masumoto A, Hirooka Y, Shimokawa H, Hironaga K, Setoguchi S, Takeshita A. Possible involvement of Rho-kinase in the pathogenesis of hypertension in humans. Hypertension 2001;38:1307–10.
24. Matoba T, Shimokawa H, Morikawa K, et al. Electron spin resonance detection of hydrogen peroxide as an endothelium-derived hyperpolarizing factor in porcine coronary microvessels. Arterioscler Thromb Vasc Biol 2003;23:1224–30.
25. Saitoh S, Zhang C, Tune JD, et al. Hydrogen peroxide: a feed-forward dilator that couples myocardial metabolism to coronary blood flow. Arterioscler Thromb Vasc Biol 2006;26:2614–21.
26. Rush JW, Laughlin MH, Woodman CR, Price EM. SOD-1 expression in pig coronary arterioles is increased by exercise training. Am J Physiol 2000;279:H2068–76.
27. Taddei S, Versari D, Cipriano A, et al. Identification of a cytochrome P450 2C9-derived endothelium- derived hyperpolarizing factor in essential hypertensive patients. J Am Coll Cardiol 2006;48:508–15.
28. Duncker DJ, Bache RJ. Regulation of coronary vasomotor tone under normal conditions and during acute myocardial hypoperfusion. Pharmacol Ther 2000;86:87–110.

Am J Physiol Heart Circ Physiol 294: H441–H448, 2008
First published November 16, 2007; doi:10.1152/ajpheart.01021.2007.

Role of Cu,Zn-SOD in the synthesis of endogenous vasodilator hydrogen peroxide during reactive hyperemia in mouse mesenteric microcirculation in vivo

Toyotaka Yada,[1] Hiroaki Shimokawa,[2] Keiko Morikawa,[3] Aya Takaki,[2] Yoshiro Shinozaki,[4] Hidezo Mori,[5] Masami Goto,[1] Yasuo Ogasawara,[1] and Fumihiko Kajiya[1]

[1]*Department of Medical Engineering and Systems Cardiology, Kawasaki Medical School, Kurashiki, Japan;* [2]*Department of Cardiovascular Medicine, Tohoku University Graduate School of Medicine, Sendai, Japan;* [3]*Department of Anesthesiology, Kyushu University Graduate School of Medical Sciences, Fukuoka, Japan;* [4]*Department of Physiology, Tokai University School of Medicine, Isehara, Japan; and* [5]*Department of Cardiac Physiology, National Cardiovascular Center Research Institute, Suita, Japan*

Submitted 4 September 2007; accepted in final form 12 November 2007

Yada T, Shimokawa H, Morikawa K, Takaki A, Shinozaki Y, Mori H, Goto M, Ogasawara Y, Kajiya F. Role of Cu,Zn-SOD in the synthesis of endogenous vasodilator hydrogen peroxide during reactive hyperemia in mouse mesenteric microcirculation in vivo. *Am J Physiol Heart Circ Physiol* 294: H441–H448, 2008. First published November 16, 2007; doi:10.1152/ajpheart.01021.2007.—We have recently demonstrated that endothelium-derived hydrogen peroxide (H_2O_2) is an endothelium-derived hyperpolarizing factor and that endothelial Cu/Zn-superoxide dismutase (SOD) plays an important role in the synthesis of endogenous H_2O_2 in both animals and humans. We examined whether SOD plays a role in the synthesis of endogenous H_2O_2 during in vivo reactive hyperemia (RH), an important regulatory mechanism. Mesenteric arterioles from wild-type and Cu,Zn-SOD$^{-/-}$ mice were continuously observed by a pencil-type charge-coupled device (CCD) intravital microscope during RH (reperfusion after 20 and 60 s of mesenteric artery occlusion) in the cyclooxygenase blockade under the following four conditions: control, catalase alone, N^G-monomethyl-L-arginine (L-NMMA) alone, and L-NMMA + catalase. Vasodilatation during RH was significantly decreased by catalase or L-NMMA alone and was almost completely inhibited by L-NMMA + catalase in wild-type mice, whereas it was inhibited by L-NMMA and L-NMMA + catalase in the Cu,Zn-SOD$^{-/-}$ mice. RH-induced increase in blood flow after L-NMMA was significantly increased in the wild-type mice, whereas it was significantly reduced in the Cu,Zn-SOD$^{-/-}$ mice. In mesenteric arterioles of the Cu,Zn-SOD$^{-/-}$ mice, Tempol, an SOD mimetic, significantly increased the ACh-induced vasodilatation, and the enhancing effect of Tempol was decreased by catalase. Vascular H_2O_2 production by fluorescent microscopy in mesenteric arterioles after RH was significantly increased in response to ACh in wild-type mice but markedly impaired in Cu,Zn-SOD$^{-/-}$ mice. Endothelial Cu,Zn-SOD plays an important role in the synthesis of endogenous H_2O_2 that contributes to RH in mouse mesenteric smaller arterioles.

nitric oxide; endothelium-derived hyperpolarizing factor; arteriole; vasodilatation

THE ENDOTHELIUM SYNTHESIZES and releases endothelium-derived relaxing factors (EDRFs), including vasodilator prostaglandins, nitric oxide (NO), and as yet unidentified endothelium-derived hyperpolarizing factor (EDHF). Since the first reports on the existence of EDHFs (4, 8), several candidates for EDHF have been proposed (9), including cytochrome *P*-450 metabolites (2, 3), endothelium-derived K^+ channel (7), and electrical communications through gap junctions between endothelial cells and vascular smooth muscle cells (34). Matoba et al. (19a, 19b, 20) previously identified that endothelium-derived hydrogen peroxide (H_2O_2) is a primary EDHF in mesenteric arteries of mice, pigs, and humans. Morikawa et al. (24a, 25) subsequently confirmed that endothelial Cu/Zn-superoxide dismutase (SOD) plays an important role in synthesizing EDHF/H_2O_2 in mice and humans. Recently, our laboratory (41a, 42) confirmed that endogenous H_2O_2 plays an important role for autoregulation and protection against reperfusion injury in canine coronary microcirculation.

Reactive hyperemia (RH) is an important regulatory mechanism of the cardiovascular system in response to a temporal reduction in blood flow for which both mechanosensitive (e.g., myogenic and shear mediated) and metabolic regulatory processes may be involved (6, 14a, 28). For the RH response of canine coronary microcirculation, NO, ATP-sensitive K^+ channels, and adenosine may all be involved (11, 41). Shear stress plays a crucial role in modulating vascular tone by stimulating the release of EDRFs (8, 32), and all three EDRFs (PGI_2, NO, and EDHF) are involved in flow-induced vasodilatation (15, 18, 33, 44).

However, it remains to be examined whether endogenous H_2O_2 is involved in the vasodilator mechanism of RH and, if so, whether endothelial Cu,Zn-SOD plays a role in the synthesis of endogenous H_2O_2 during RH. The present study was thus designed to address these important issues in mice. Our laboratory (42, 44) previously reported that the contribution of EDHF to the vasodilatory mechanisms increases as the diameter of the vessel decreases. Thus, by employing a pencil-type charge-coupled device (CCD) intravital microscope with a high resolution, we focused on the arterioles with a diameter of <50 μm in vivo.

METHODS

The present study was approved by the Animal Care and Use Committee of Kawasaki Medical School and conformed to the guidelines on animal experiments of Kawasaki Medical School and *the*

Address for reprint requests and other correspondence: Toyotaka Yada, Dept. of Medical Engineering and Systems Cardiology, Kawasaki Medical School, 577 Matsushima, Kurashiki, Okayama 701-0192 Japan (e-mail: yada@me.kawasaki-m.ac.jp).

The costs of publication of this article were defrayed in part by the payment of page charges. The article must therefore be hereby marked "*advertisement*" in accordance with 18 U.S.C. Section 1734 solely to indicate this fact.

Guide for the Care and Use of Laboratory Animals published by the National Institutes of Health.

Animal preparation. Male Cu,Zn-SOD$^{-/-}$ and control mice (10–16 wk of age) derived from breeding pairs of heterozygous (Cu,Zn-SOD$^{+/-}$) mice (Jackson Laboratory, Bar Harbor, ME) were used (25). They were placed on a heating blanket to maintain body temperature at 37°C throughout the experiment. The animals were anesthetized with 1% inhalational anesthesia of isoflurane. After tracheal intubation, they were ventilated with a mixture of room air and oxygen by a ventilator. The abdomen was opened, and a 24-Fr catheter was inserted into the abdominal aorta to measure aortic pressure. Mesenteric arterioles were continuously observed by a pencil-type intravital microscope (Nihon Kohden, Tokyo, Japan) (13).

Measurements of diameter by pencil-type intravital microscope. Mesenteric arterioles were visualized using a pencil-type intravital microscope (13). The system was modified for the visualization of microcirculation from our previous needle-probe CCD videomicroscope system (40). The microscopic images were monitored and recorded on a digital videocassette recorder (Sony, Tokyo, Japan) every 33 ms (30 frames/s). The spatial resolution of a static image of this system is 0.5 μm for ×600 magnification. The field of view is 367 × 248 μm, and the focal depth is 50 μm.

Measurements of regional blood flow in mesenteric arteries. Regional blood flow in mesenteric arteries was measured by the nonradioactive microsphere (15 μm; Sekisui Plastic, Tokyo, Japan) technique at the end of the experiments, as previously described (24). Briefly, a bolus (50 μl) of the microspheres suspension (5×10^5 spheres; Ce and Ba) were injected into the abdominal aorta at baseline and 5 s after the reperfusion of the mesenteric artery with confirming changes of the blood flow of the mesenteric artery by a CCD intravital microscope and without inducing hemodynamic changes (14). Mice were euthanized, and the mesenterium was extracted. The X-ray fluorescence of the stable heavy elements was measured by a wavelength-dispersive spectrometer (model PW 1480; Phillips, Eindhoven, the Netherlands). The relative increase in blood flow of mesenterium [microsphere count/tissue weight (g)] during RH from baseline was calculated.

Detection of H_2O_2 and NO production in mesenteric microvessels. 2′,7′-Dichlorodihydrofluorescein diacetate (DCF-DA; Molecular Probes, Eugene, OR) and diaminorhodamine-4M AM (DAR; Daiichi Pure Chemicals, Tokyo, Japan) were used to detect H_2O_2 and NO production in mesenteric microvessels, respectively, as previously described (41a). Briefly, fresh and unfixed mesenteric tissue was cut into several blocks and immediately frozen in an optimal cutting temperature compound (Tissue-Tek; Sakura Fine Chemical, Tokyo, Japan). After washout of the mesenteric tissue with phosphate-buffered solution under a normal temperature, fluorescent images of the microvessels were obtained 3 min after application of acetylcholine (ACh) by using a fluorescence microscope (Olympus BX51) (41a). We defined the baseline fluorescent intensity as the response in the vascular endothelium just after the injection of NO or H_2O_2 fluorescent dye. The fluorescence data at baseline (both DCF-DA and DAR) were obtained after the RH.

Experimental protocol. We performed four protocols. First, mesenteric arterioles in wild-type and Cu,Zn-SOD$^{-/-}$ mice were continuously observed by a pencil-type intravital microscope during RH (reperfusion after 20 and 60 s of mesenteric artery occlusion) with cyclooxygenase blockade [indomethacin, 5×10^{-5} mol/l topical administration (ta)] with the following four conditions: control, catalase alone [1,500 U·min^{-1}·100 g body wt^{-1} intra-arterial administration (ia) polyethylene glycol-catalase, a specific decomposer of H_2O_2], NO synthase inhibitor alone (10^{-4} mol/l ta L-NMMA), and L-NMMA + catalase (17). In the presence of indomethacin and L-NMMA, microspheres were administered at baseline and 5 s after the reperfusion into the abdominal aorta by bolus injection because RH peaked within 20–60 s after release from 20- and 60-s occlusion (29). Maximal vascular diameter was measured within 20 and 60 s after the reperfusion. Second, ACh (10^{-7} to 10^{-5} mol/l ta)-induced endothelium-dependent vasodilatation was examined under the control conditions and in the presence of Tempol, a SOD mimetic 4-hydroxy-2,2,6,6-tetramethylpiperidine-*N*-oxyl (50 μg·min^{-1}·100 g body wt^{-1} ia) (17), and Tempol + catalase. In the combined infusion protocol (Tempol or Tempol + catalase) in the presence of cyclooxygenase blockade + L-NMMA, the combined infusion was performed simultaneously for 20 min, ACh was infused for 10 min, and the vascular diameter was measured. Third, sodium nitroprusside (SNP; 10^{-7} to 10^{-5} mol/l ta, each 10 min)-induced endothelium-independent vasodilatation was examined in wild-type and Cu,Zn-SOD$^{-/-}$ mice. Fourth, fresh and unfixed mesenteric tissue was then cut into several blocks and immediately frozen in optimal cutting temperature compound.

Statistical analysis. The results are expressed as means ± SE. Dose-response curves were analyzed by two-way ANOVA followed by the Scheffé's post hoc test for multiple comparisons. Vascular responses were analyzed by one-way ANOVA followed by the Scheffé's post hoc test for multiple comparisons. $P < 0.05$ was considered to be statistically significant.

RESULTS

Hemodynamics and blood gases during RH. Throughout the experiments, mean aortic pressure and heart rate were constant and comparable (Tables 1 and 2), and Po_2, Pco_2, and pH were maintained within the physiological ranges (>70 mmHg Po_2, 25–40 mmHg Pco_2, and pH 7.35–7.45). Baseline mesenteric

Table 1. *Hemodynamics during RH*

		Control		Catalase		L-NMMA		L-NMMA + Catalase	
	n	B	RH	B	RH	B	RH	B	RH
MBP, RH 20, mmHg									
WT	10	83±7	85±9	81±7	82±7	82±8	81±6	83±8	82±6
Cu/Zn-SOD$^{-/-}$	10	85±12	87±10	83±8	82±8	82±8	82±8	82±8	80±9
MBP, RH 60, mmHg									
WT	5	86±8	88±7	87±7	88±7	88±8	87±7	88±7	87±7
Cu/Zn-SOD$^{-/-}$	5	88±8	86±8	87±6	89±9	88±7	88±8	89±6	90±11
HR, RH 20, beats/min									
WT	10	346±14	348±14	335±15	333±17	315±15	310±17	330±18	330±18
Cu/Zn-SOD$^{-/-}$	10	364±27	354±22	350±18	351±15	355±15	340±17	355±15	335±17
HR, RH 60, beats/min									
WT	5	351±31	361±9	353±21	356±13	358±10	364±37	354±22	355±15
Cu/Zn-SOD$^{-/-}$	5	346±18	356±25	356±15	361±19	351±31	361±9	358±10	364±27

Values are means ± SE; *n*, number of rats. RH, reactive hyperemia; L-NMMA, N^G-monomethyl-L-arginine; B, baseline; MBP, mean blood pressure; HR, heart rate; WT, wild-type.

Table 2. *Hemodynamics during administration of ACh and SNP*

		Control				Tempol			Tempol + Catalase			SNP			
	n	B	ACh 10^{-7}	ACh 10^{-6}	ACh 10^{-5}	ACh 10^{-7}	ACh 10^{-6}	ACh 10^{-5}	ACh 10^{-7}	ACh 10^{-6}	ACh 10^{-5}	B	SNP 10^{-7}	SNP 10^{-6}	SNP 10^{-5}
MBP, mmHg															
WT	10	90±7	88±7	87±7	89±6	91±10	90±11	84±11	91±8	86±8	86±8	78±13	77±13	76±13	76±13
Cu/Zn-SOD$^{-/-}$	10	93±11	92±10	94±10	97±10	98±16	97±15	99±15	91±8	91±8	88±8	81±8	77±10	75±11	74±11
HR, beats/min															
WT	10	361±9	340±17	340±17	340±17	342±24	336±25	336±25	320±19	330±27	330±27	370±57	364±37	351±31	351±31
Cu/Zn-SOD$^{-/-}$	10	386±11	381±24	371±21	396±13	386±11	377±15	377±15	362±22	356±25	356±25	372±21	369±6	358±10	346±18

Values are means ± SE; n, number of rats. SNP, sodium nitroprusside; ACh, acetylcholine.

arteriolar diameter was comparable in the absence and presence of inhibitors under the four different experimental conditions (Tables 3 and 4). Those different inhibitors (L-NMMA, catalase, and Tempol) did not affect basal diameter.

Mesenteric vasodilatation during RH. We were able to observe EDHF-sensitive smaller arterioles (18–66 μm) by using a newly developed pencil-type CCD intravital microscope with a higher resolution. In the mesenteric arterioles of wild-type mice, vasodilatation during RH to 20- and 60-s arterial occlusion was decreased by catalase or L-NMMA alone and was almost completely inhibited by L-NMMA + catalase (Fig. 1). In contrast, in mesenteric arterioles of Cu,Zn-SOD$^{-/-}$ mice, vasodilatation during RH to 20- and 60-s arterial occlusion was decreased by catalase alone and was almost completely inhibited by L-NMMA alone or L-NMMA + catalase (Fig. 1). Blood flow measurement by microsphere technique showed that in the presence of indomethacin and L-NMMA, RH-induced increase in blood flow was 232 ± 4% (20 s) and 331 ± 4% (60 s) of baseline in control and was sensitive to catalase (137 ± 4%, 20 s; and 147 ± 17%, 60 s) in the wild-type mice, whereas in the Cu,Zn-SOD$^{-/-}$ mice, the vasodilator response was significantly reduced to 125 ± 19% (20 s) and 145 ± 23% (60 s) in control and was insensitive to catalase (120 ± 24%, 20 s; and 139 ± 19%, 60 s) (Fig. 2). With the longer occlusion of the mesenteric artery, the shear stimulus for H_2O_2 release was significantly increased in the control condition and was significantly decreased by catalase.

Endothelium-dependent vasodilatation. In mesenteric arterioles of wild-type mice, endothelium-dependent vasodilatation to ACh (10^{-7} to 10^{-5} mol/l in the presence of indomethacin and L-NMMA) was unchanged with Tempol but significantly inhibited by the addition of catalase (Fig. 3). In contrast, in the mesenteric arterioles of the Cu,Zn-SOD$^{-/-}$ mice, the response to ACh was significantly enhanced with Tempol, a response that was sensitive to the addition of catalase (Fig. 3).

Endothelium-independent vasodilatation. Endothelium-independent vasodilatation to SNP (10^{-7} to 10^{-5} mol/l in the presence of L-NMMA + catalase) was comparable between the two strains (Table 4).

Detection of H_2O_2 and NO production in the mesenteric artery. Fluorescent microscopy with DCF-DA showed that vascular H_2O_2 production in mesenteric arterioles was significantly increased in response to ACh in wild-type mice compared with baseline but markedly impaired in Cu,Zn-SOD$^{-/-}$ mice (Fig. 4). In contrast, vascular NO production in mesenteric arterioles, as assessed by DAR fluorescent intensity, was significantly increased in response to ACh in wild-type mice compared with baseline and was unaltered in Cu,Zn-SOD$^{-/-}$ mice (Fig. 5).

DISCUSSION

The novel finding of the present study with a newly developed pencil-type CCD intravital microscope in vivo is that Cu,Zn-SOD plays an important role in the synthesis of endogenous H_2O_2, which is substantially involved in the mechanisms of RH-induced vasodilatation in mouse mesenteric circulation.

Impaired EDHF-mediated vasodilatation in Cu,Zn-SOD$^{-/-}$ mice in vivo. Matoba et al. (19a, 20) have previously identified that endothelium-derived H_2O_2 is an EDHF in mouse and

Table 3. *Diameter change during RH*

	Control		Catalase		L-NMMA		L-NMMA + Catalase	
	B	RH	B	RH	B	RH	B	RH
RH 20, μm								
WT	36±4	49±4†	36±4	44±4†	36±3	42±3*	36±4	38±3
Cu/Zn-SOD$^{-/-}$	36±4	48±5†	36±4	42±5†	36±4	38±4	36±3	38±4
RH 60, μm								
WT	40±4	55±4†	40±4	51±4†	40±5	47±4*	39±4	41±4
Cu/Zn-SOD$^{-/-}$	40±3	56±4†	40±3	51±4†	39±4	42±3	40±5	42±3

Values are means ± SE; *n*, number of arterioles per animal. *$P < 0.01$ vs. B.

human mesenteric microvessels. Subsequently, our laboratory (42) and others (23) have confirmed that endogenous H_2O_2 exerts important vasodilator effects in canine coronary microcirculation in vivo and in isolated human coronary microvessels, respectively. H_2O_2 can be formed from superoxide anions derived from several sources in endothelial cells, including endothelial NO synthase (eNOS), cyclooxygenase, lipoxygenase, cytochrome *P*-450 enzymes, and reduced NADP [NAD(P)H] oxidases. Gupte et al. (10) demonstrated that cytosolic NADH redox and Cu,Zn-SOD activity have important roles in controlling the inhibitory effects of superoxide anions derived from NADH oxidase. Morikawa et al. (24a, 25) have also demonstrated that endothelial Cu,Zn-SOD plays an important role in the synthesis of H_2O_2 in mouse and human mesenteric arteries in vitro.

In the present study, catalase or L-NMMA alone significantly, but not completely, inhibited the RH-induced vasodilatation of mesenteric arterioles in wild-type mice in vivo, whereas L-NMMA + catalase markedly attenuated the remaining vasodilatation. In contrast, in Cu,Zn-SOD$^{-/-}$ mice, L-NMMA alone significantly decreased the vasodilatation and blood flow in response to 20- and 60-s arterial occlusion (Figs. 1 and 2). These results obtained using a pencil-type CCD intravital microscope indicate that H_2O_2 exerts important vasodilator effects on mesenteric smaller arterioles during RH and that Cu,Zn-SOD plays an important role in the synthesis of endogenous H_2O_2 during RH in vivo. Koller and Bagi (14a) showed that RH in rat isolated coronary arterioles was sensitive to pressure/stretch and flow/shear stress. Miura et al. (23) also showed the important role of endogenous H_2O_2 in flow-induced vasodilatation of human coronary arterioles. Koller and Bagi (14a) also suggested that H_2O_2 contributes to the development of the early peak phase of RH but not the duration of reactive vasodilatation, whereas NO prolongs the later phase of RH in rat isolated coronary arterioles, suggesting that H_2O_2 released endogenously within the vascular wall changes hemodynamic forces. In the present study, peak blood flow was significantly decreased after catalase (Fig. 2), suggesting that flow-induced vasodilatation during the early phase of RH is indeed mediated by H_2O_2 in mouse mesenteric arterioles in vivo.

Compensatory vasodilator mechanism between H_2O_2 and NO. It is well known that coronary vascular tone is regulated by the interactions among hemodynamic forces and several endogenous vasodilators, including NO, H_2O_2, and adenosine (41a, 42). Koller and Bagi (14a) demonstrated that mechanosensitive mechanisms were activated by changes in pressure and flow/shear stress during RH in isolated coronary arterioles. A superoxide anion is dismutated to H_2O_2 by manganese SOD (Mn-SOD, mitochondrial matrix) and Cu,Zn-SOD. H_2O_2 diffuses across the mitochondrial membrane to act on vascular smooth muscle (45). Tsunoda et al. (35) demonstrated that Mn-SOD augmented RH during 60-s canine coronary ischemia and reperfusion. H_2O_2 generated in the arteriolar smooth muscle could cause the response of activation of cGMP in rat skeletal muscle arterioles (38). Kitakaze et al. (12) indicated that the augmentation of reactive hyperemic flow caused by SOD is attributed to the enhanced release of adenosine in canine coronary circulation. These endogenous vasodilators may play an important role in causing the compensatory vasodilatation of coronary microvessels during myocardial ischemia.

In the present study, endothelium-dependent vasodilatation during RH (in the presence of L-NMMA) was almost completely inhibited by catalase in wild-type mice. In the Cu,Zn-SOD$^{-/-}$ mice, vasodilatation during RH remained under the control condition but was almost completely inhibited by L-NMMA (Fig. 1). The RH-induced increase in blood flow (in the presence of indomethacin and L-NMMA) was significantly inhibited by catalase in the wild-type mice but not in Cu,Zn-SOD$^{-/-}$ mice (Fig. 2). RH-induced increase in blood flow (in the presence of indomethacin and L-NMMA) remained in Cu,Zn-SOD$^{-/-}$ mice (Fig. 2). H_2O_2 may compensate for the loss of action of NO. H_2O_2 produced by SOD other than Cu,Zn-SOD may compensate for the loss of action of Cu,Zn-SOD-derived H_2O_2.

Table 4. *Diameter change during administration of ACh and SNP*

	ACh				SNP			
	B	ACh 10^{-7}	ACh 10^{-6}	ACh 10^{-5}	B	SNP 10^{-7}	SNP 10^{-6}	SNP 10^{-5}
WT, μm	36±3	41±3*	45±3†	49±4†	35±4	39±4*	43±5†	46±5†
Cu/Zn-SOD$^{-/-}$, μm	36±4	38±4	41±4*	44±4†	34±4	38±4*	41±4†	44±4†

Values are means ± SE; *n*, number of arterioles per animal. *$P < 0.05$; †$P < 0.01$ vs. B.

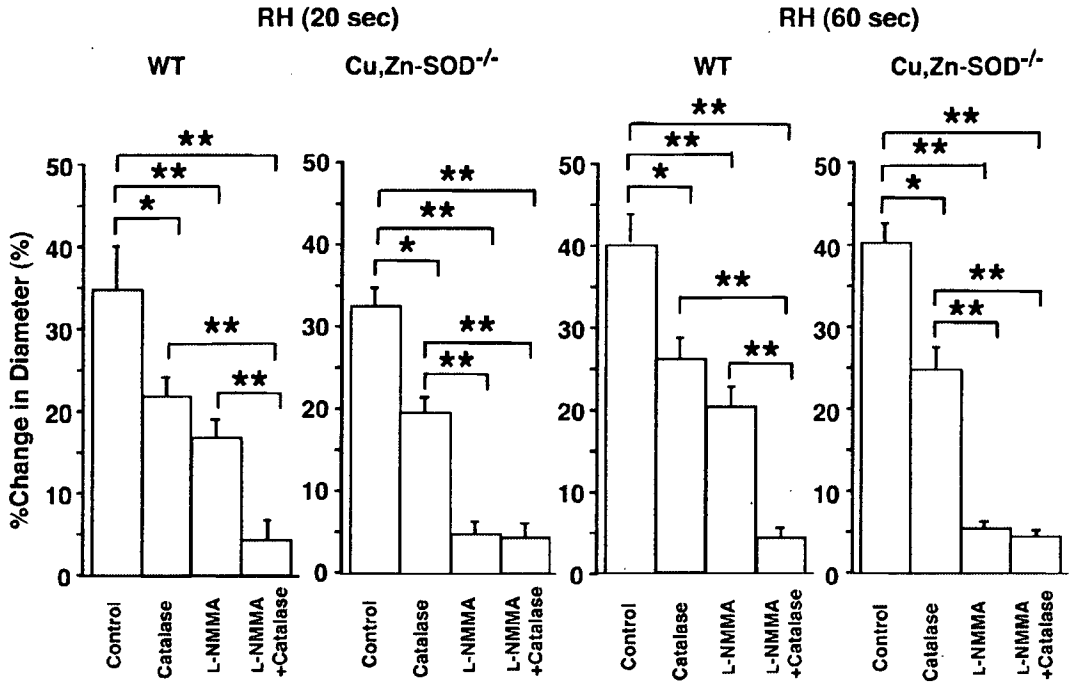

Fig. 1. Mesenteric vasodilatation during reactive hyperemia (RH). In the wild-type (WT) mice, vasodilatation during RH was inhibited by catalase or N^{ω}-monomethyl-L-arginine (L-NMMA) and further inhibited by L-NMMA + catalase. In the Cu,Zn-SOD$^{-/-}$ mice (Cu,Zn-SOD$^{-/-}$), vasodilatation during RH was inhibited by catalase and markedly inhibited by L-NMMA, and the remaining response was not inhibited by catalase. The number of arterioles per animals used was 10/5 for each group. *$P < 0.05$; **$P < 0.01$.

Improvement of ACh-induced vasodilatation by Tempol in Cu,Zn-SOD$^{-/-}$ mice. It was previously reported that Tempol, a cell membrane-permeable SOD mimetic 4-hydroxy-2,2,6,6-tetramethylpiperidine-*N*-oxyl, decreased oxidative stress in the spontaneously hypertensive rat (31). In the present study, Tempol significantly improved the ACh-induced vasodilatation in Cu,Zn-SOD$^{-/-}$ mice, whereas catalase abolished the beneficial effect of Tempol (Fig. 3), indicating that the effect of Tempol was mediated by endogenous H_2O_2 in vivo. In contrast, Tempol had no enhancing effect on the ACh-induced vasodilatation in control mice (Fig. 3), suggesting that a sufficient amount of SOD is present in this strain. In Cu,Zn-SOD$^{-/-}$ mice, L-NMMA did not abolish the ACh-induced vasodilation, and the DCF-DA stain showed remaining fluorescent intensity (Fig. 4). Thus the residual vasodilatation could be caused by the following possible mechanisms. First, NO may also be synthesized in a nonenzymatic manner (27). Nonenzymatic synthesis of NO could occur in the presence of NADPH, glutathione, and L-cysteine, etc., opposing the effects of NOS inhibition (27). Second, the effects of L-NMMA may be limited since it is known that L-NMMA does not abolish NO production (1). H_2O_2 produced from vascular smooth muscle cells and other tissues may also contribute to the residual vasodilation (5, 30). Third, the contribution of other proposed

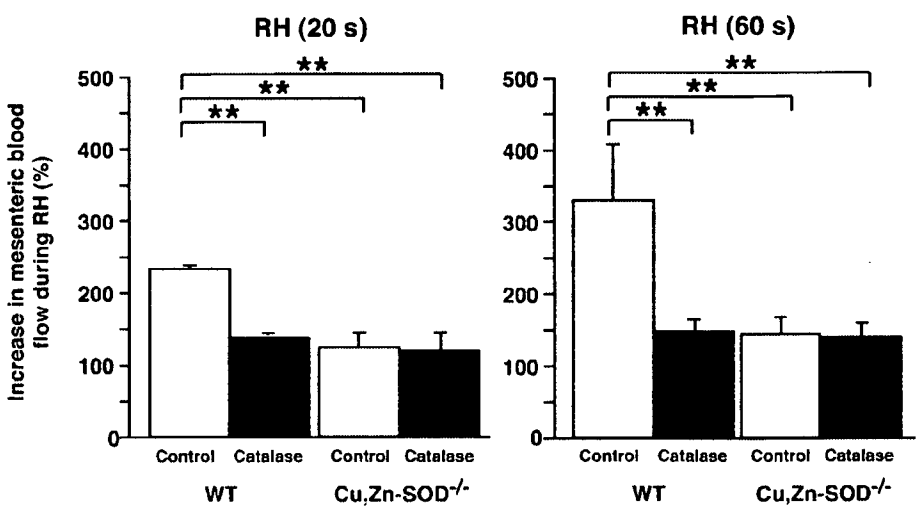

Fig. 2. The increase in mesenteric blood flow during RH. In the presence of indomethacin and L-NMMA, RH-induced increase in blood flow was sensitive to catalase in the WT mice, whereas in the Cu,Zn-SOD$^{-/-}$, the vasodilation was significantly reduced in control and was insensitive to catalase. The number of animals used was 5 for each group. **$P < 0.01$.

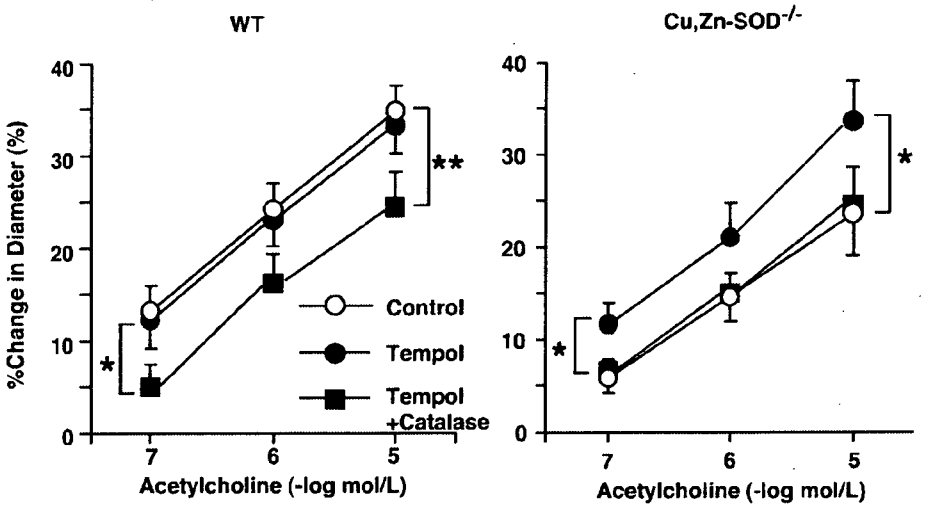

Fig. 3. Endothelium-dependent relaxations to ACh. In the WT mice, endothelium-dependent vasodilatation to ACh (in the presence of indomethacin and L-NMMA) was unchanged with Tempol but significantly inhibited by the addition of catalase. In the Cu,Zn-SOD$^{-/-}$, the vasodilation was significantly enhanced with Tempol, where the response was sensitive to the addition of catalase. The number of arterioles per animals used was 10/5 for each group. *P < 0.05; **P < 0.01.

EDHF candidates, such as P-450 metabolites (2, 3) and potassium ion (7), may contribute to the residual vasodilatation. Although RH and ACh have different mechanisms of vasodilator effects, they also share the same flow-induced vasodilator mechanism.

Endothelium-independent vasodilatation in Cu,Zn-SOD$^{-/-}$ mice. Microvascular dysfunction in hypercholesterolemic rats was confined to the endothelium because the dilator response to SNP and adenosine was unchanged (37). In the present study, endothelium-independent vasodilatation in response to SNP was comparable between the two genotypes, suggesting that vasodilatation properties of vascular smooth muscle cells were preserved in the Cu,Zn-SOD$^{-/-}$ mice in vivo.

Detection of vascular H_2O_2 and NO production. Our laboratory (41a) has recently demonstrated that vascular production of H_2O_2 and NO after ischemia-reperfusion is enhanced in small coronary arteries and arterioles in vivo, respectively. It was previously shown that a ACh-induced increase in fluorescence intensity in endothelial cells of the mesenteric artery is significantly reduced in Cu,Zn-SOD$^{-/-}$ mice (25). In the present study, vascular H_2O_2 production, as assessed by DCF-DA fluorescent intensity in mesenteric arterioles, was markedly impaired

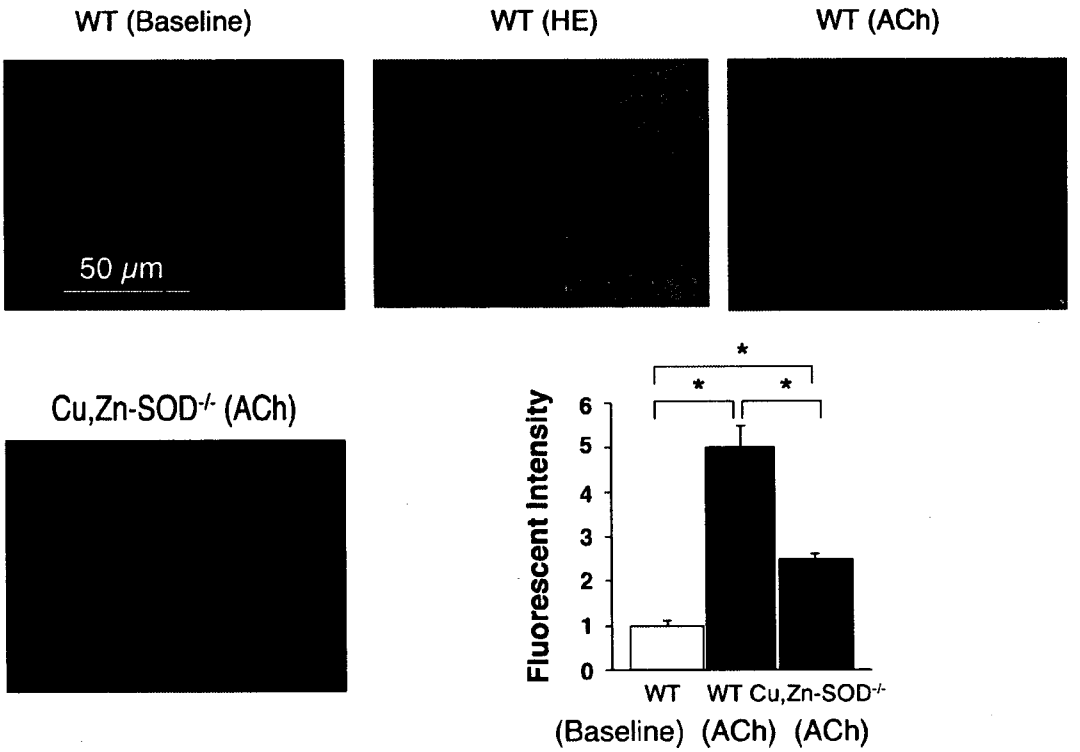

Fig. 4. Detection of vascular H_2O_2 production. Vascular H_2O_2 production in mesenteric arterioles was significantly increased in response to ACh in WT mice but markedly impaired in Cu,Zn-SOD$^{-/-}$. The number of arterioles per animals used was 10/5 for each group. *P < 0.05. HE, Hematoxylin eosin.

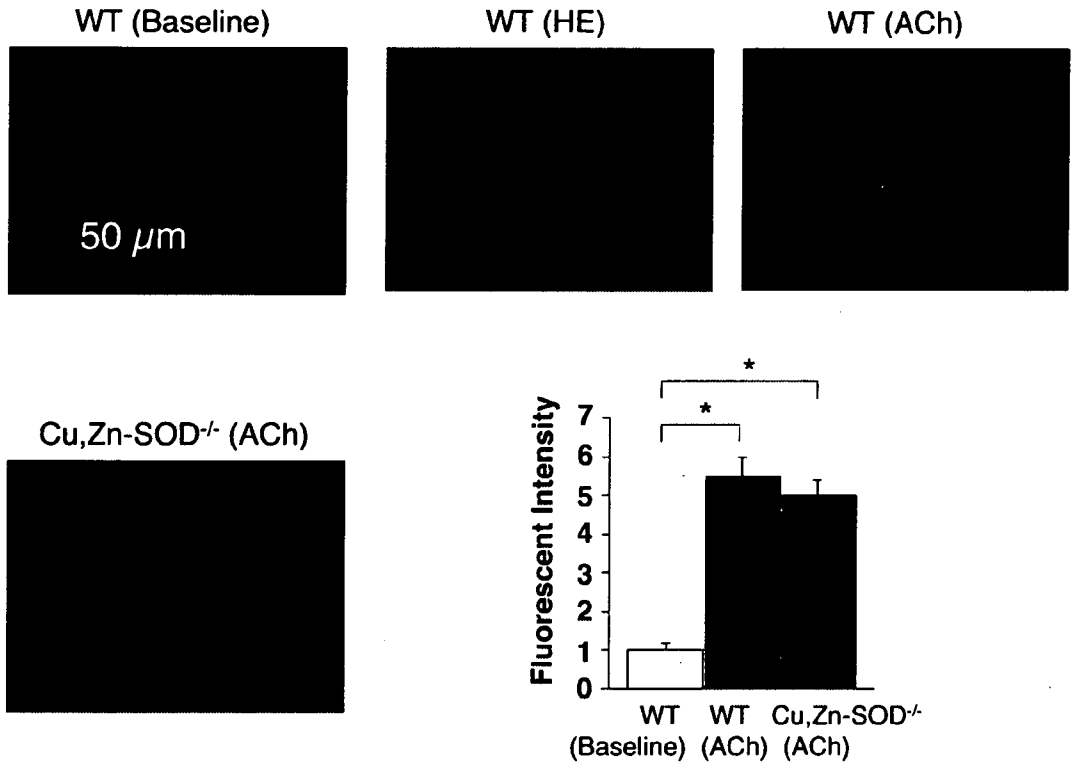

Fig. 5. Detection of vascular nitric oxide (NO) production. Vascular NO production in mesenteric arterioles was significantly increased in response to ACh in WT mice and unaltered in Cu,Zn-SOD$^{-/-}$. The number of arterioles per animals used was 10/5 for each group. *$P < 0.05$.

in Cu,Zn-SOD$^{-/-}$ mice (Fig. 4). These findings indicate that endothelial production of H_2O_2 is significantly impaired in Cu,Zn-SOD$^{-/-}$ mice, confirming the importance of the enzyme in endothelial synthesis of H_2O_2.

In the previous study by Morikawa et al. (25), eNOS protein expression was comparable between Cu,Zn-SOD$^{-/-}$ and wild-type mice. In the present study, vascular NO production in small mesenteric artery was unaltered in Cu,Zn-SOD$^{-/-}$ mice compared with wild-type mice (Fig. 5). NO could compensate for the loss of action of H_2O_2, although there are still many uncertainties about the local cellular dynamics of superoxide anions and NO.

Study limitations. Several limitations should be mentioned for the present study. First, we estimated blood flow in the mesenteric circulation using microspheres. We were unable to calculate the absolute values of local blood flow or shear stress because of the methodological limitations. However, since the flow measurement with microspheres was performed at the end of the experiments, it should not have influenced other results. Second, we used Cu,Zn-SOD$^{-/-}$ mice in the present study, where unknown compensatory mechanisms may be operative, and we were unable to elucidate the mechanism(s) for the remaining EDHF-mediated responses in those mice.

Clinical implications. RH is an important regulatory mechanism of the cardiovascular system, reflecting the flow reserve in response to a brief period of cessation of flow. An impaired flow reserve in resistance vessels is a hallmark of microvascular dysfunction with coronary risk factors. Hypertension is associated with structural alterations in the microcirculation and a reduced endothelium-dependent dilation in conduit arteries (19). It is well known that abnormality in Cu,Zn-SOD is noted in several diseases, including hypertension and diabetes mellitus (36, 39).

In conclusion, endogenous H_2O_2 exerts important vasodilator effects of mesenteric smaller arterioles during RH, especially at the low level of NO, and that Cu,Zn-SOD plays an important role in the synthesis of endogenous H_2O_2 during RH in vivo.

GRANTS

This work was supported in part by the Japanese Ministry of Education, Science, Sports, Culture, and Technology (Tokyo, Japan) Grants 16209027 (to H. Shimokawa), 16300164, and 19300167 (to T. Yada), the Program for Promotion of Fundamental Studies in Health Sciences of the Organization for Pharmaceutical Safety and Research of Japan (to H. Shimokawa), and Takeda Science Foundation 2002 (to T. Yada).

REFERENCES

1. **Amezcua JL, Palmer RM, de Souza BM, Moncada S.** Nitric oxide synthesized from L-arginine regulates vascular tone in the coronary circulation of the rabbit. *Br J Pharmacol* 97: 1119–1124, 1989.
2. **Bauersachs J, Hecker M, Busse R.** Display of the characteristics of endothelium-derived hyperpolarizing factor by a cytochrome P450-derived arachidonic acid metabolite in the coronary microcirculation. *Br J Pharmacol* 113: 1548–1553, 1994.
3. **Campbell WB, Gebremedhin D, Pratt PF, Harder DR.** Identification of epoxyeicosatrienoic acids as an endothelium-derived hyperpolarizing factor. *Circ Res* 78: 415–423, 1996.
4. **Chen G, Suzuki H, Weston AH.** Acetylcholine releases endothelium-derived hyperpolarizing factor and EDRF from blood vessels. *Br J Pharmacol* 95: 1165–1174, 1988.
5. **Chen Y, Pearlman A, Luo Z, Wilcox CS.** Hydrogen peroxide mediates a transient vasorelaxation with Tempol during oxidative stress. *Am J Physiol Heart Circ Physiol* 293: H2085–H2092, 2007.

6. **Coffman JD, Gregg DE.** Reactive hyperemia characteristics of the myocardium. *Am J Physiol* 199: 1143–1149, 1960.
7. **Edwards G, Dora KA, Gardener MJ, Garland CJ, Weston AH.** K^+ is an endothelium-derived hyperpolarizing factor in rat arteries. *Nature* 396: 269–272, 1998.
8. **Feletou M, Vanhoutte PM.** Endothelium-dependent hyperpolarization of canine smooth muscle. *Br J Pharmacol* 93: 515–524, 1988.
9. **Feletou M, Vanhoutte PM.** Endothelium-derived hyperpolarizing factor: where are we now? *Arterioscler Thromb Vasc Biol* 26: 1215–1225, 2006.
10. **Gupte SA, Rupawalla T, Mohazzab-H KM, Wolin MS.** Regulation of NO-elicited pulmonary artery relaxation and guanylate cyclase activation by NADH oxidase and SOD. *Am J Physiol Heart Circ Physiol* 276: H1535–H1542, 1999.
11. **Kanatsuka H, Sekiguchi N, Sato K, Akai K, Wang Y, Komaru T, Ashikawa K, Takishima T.** Microvascular sites and mechanisms responsible for reactive hyperemia in the coronary circulation of the beating canine heart. *Circ Res* 71: 912–922, 1992.
12. **Kitakaze M, Hori M, Takashima S, Iwai K, Sato H, Inoue M, Kitabatake A, Kamada T.** Superoxide dismutase enhances ischemia-induced reactive hyperemic flow and adenosine release in dogs. A role of 5′-nucleotidase activity. *Circ Res* 71: 558–566, 1992.
13. **Kiyooka T, Hiramatsu O, Shigeto F, Nakamoto H, Tachibana H, Yada T, Ogasawara Y, Kajiya M, Morimoto T, Morizane Y, Mohri S, Shimizu J, Ohe T, Kajiya F.** Direct observation of epicardial coronary capillary hemodynamics during reactive hyperemia and during adenosine administration by intravital video microscopy. *Am J Physiol Heart Circ Physiol* 288: H1437–H1443, 2005.
14. **Kobayashi N, Kobayashi K, Kouno K, Horinaka S, Yagi S.** Effects of intra-atrial injection of colored microspheres on systemic hemodynamics and regional blood flow in rats. *Am J Physiol Heart Circ Physiol* 266: H1910–H1917, 1994.

14a. **Koller A, Bagi Z.** Nitric oxide and H_2O_2 contribute to reactive dilation of isolated coronary arterioles. *Am J Physiol Heart Circ Physiol* 287: H2461–H2467, 2004.

15. **Koller A, Sun D, Kaley G.** Role of shear stress and endothelial prostaglandins in flow- and viscosity-induced dilation of arterioles in vitro. *Circ Res* 72: 1276–1284, 1993.
17. **Kopkan L, Castillo A, Navar LG, Majid DS.** Enhanced superoxide generation modulates renal function in ANG II-induced hypertensive rats. *Am J Physiol Renal Physiol* 290: F80–F86, 2006.
18. **Kuo L, Davis MJ, Chilian WM.** Endothelium-dependent, flow-induced dilation of isolated coronary arterioles. *Am J Physiol Heart Circ Physiol* 259: H1063–H1070, 1990.
19. **Lauer T, Heiss C, Preik M, Balzer J, Hafner D, Strauer BE, Kelm M.** Reduction of peripheral flow reserve impairs endothelial function in conduit arteries of patients with essential hypertension. *J Hypertens* 23: 563–569, 2005.

19a. **Matoba T, Shimokawa H, Kubota H, Morikawa K, Fujiki T, Kunihiro I, Mukai Y, Hirakawa Y, Takeshita A.** Hydrogen peroxide is an endothelium-derived hyperpolarizing factor in human mesenteric arteries. *Biochem Biophys Res Commun* 290: 909–913, 2002.

19b. **Matoba T, Shimokawa H, Morikawa K, Kubota H, Kunihiro I, Urakami-Harasawa L, Mukai Y, Hirakawa Y, Akaike T, Takeshita A.** Electron spin resonance detection of hydrogen peroxide as an endothelium-derived hyperpolarizing factor in porcine coronary microvessels. *Arterioscler Thromb Vasc Biol* 23: 1224–1230, 2003.

20. **Matoba T, Shimokawa H, Nakashima M, Hirakawa Y, Mukai Y, Hirano K, Kanaide H, Takeshita A.** Hydrogen peroxide is an endothelium-derived hyperpolarizing factor in mice. *J Clin Invest* 106: 1521–1530, 2000.
23. **Miura H, Bosnjak JJ, Ning G, Saito T, Miura M, Gutterman DD.** Role for hydrogen peroxide in flow-induced dilation of human coronary arterioles. *Circ Res* 92: e31–e40, 2003.
24. **Mori H, Haruyama S, Shinozaki Y, Okino H, Iida A, Takanashi R, Sakuma I, Husseini WK, Payne BD, Hoffman JI.** New nonradioactive microspheres and more sensitive X-ray fluorescence to measure regional blood flow. *Am J Physiol Heart Circ Physiol* 263: H1946–H1957, 1992.

24a. **Morikawa K, Fujiki T, Matoba T, Kubota H, Hatanaka M, Takahashi S, Shimokawa H.** Important role of superoxide dismutase in EDHF-mediated responses of human mesenteric arteries. *J Cardiovasc Pharmacol* 44: 552–556, 2004.

25. **Morikawa K, Shimokawa H, Matoba T, Kubota H, Akaike T, Talukder MA, Hatanaka M, Fujiki T, Maeda H, Takahashi S, Takeshita A.** Pivotal role of Cu,Zn-superoxide dismutase in endothelium-dependent hyperpolarization. *J Clin Invest* 112: 1871–1879, 2003.
27. **Moroz LL, Norby SW, Cruz L, Sweedler JV, Gillette R, Clarkson RB.** Non-enzymatic production of nitric oxide (NO) from NO synthase inhibitors. *Biochem Biophys Res Commun* 253: 571–576, 1998.
28. **Olsson RA.** Myocardial reactive hyperemia. *Circ Res* 37: 263–270, 1975.
29. **Pawlik WW, Obuchowicz R, Pawlik MW, Sendur R, Biernat J, Brzozowski T, Konturek SJ.** Histamine H_3 receptors modulate reactive hyperemia in rat gut. *J Physiol Pharmacol* 55: 651–661, 2004.
30. **Saitoh S, Zhang C, Tune JD, Potter B, Kiyooka T, Rogers PA, Knudson JD, Dick GM, Swafford A, Chilian WM.** Hydrogen peroxide: a feed-forward dilator that couples myocardial metabolism to coronary blood flow. *Arterioscler Thromb Vasc Biol* 26: 2614–2621, 2006.
31. **Schnackenberg CG, Wilcox CS.** Two-week administration of Tempol attenuates both hypertension and renal excretion of 8-Iso prostaglandin F_{2alpha}. *Hypertension* 33: 424–428, 1999.
32. **Shimokawa H.** Primary endothelial dysfunction: atherosclerosis. *J Mol Cell Cardiol* 31: 23–37, 1999.
33. **Takamura Y, Shimokawa H, Zhao H, Igarashi H, Egashira K, Takeshita A.** Important role of endothelium-derived hyperpolarizing factor in shear stress-induced endothelium-dependent relaxations in the rat mesenteric artery. *J Cardiovasc Pharmacol* 34: 381–387, 1999.
34. **Taylor HJ, Chaytor AT, Evance WH, Griffith TM.** Inhibition of the gap junctional component of endothelium-dependent relaxations in rabbit iliac artery by 18-alpha glycyrrhetinic acid. *Br J Pharmacol* 125: 1–3, 1998.
35. **Tsunoda R, Okumura K, Ishizaka H, Matsunaga T, Tabuchi T, Tayama S, Yasue H.** Enhancement of myocardial reactive hyperemia with manganese-superoxide dismutase: role of endothelium-derived nitric oxide. *Cardiovasc Res* 31: 537–545, 1996.
36. **Uchimura K, Nagasaka A, Hayashi R, Makino M, Nagata M, Kakizawa H, Kobayashi T, Fujiwara K, Kato T, Iwase K, Shinohara R, Kato K, Itoh M.** Changes in superoxide dismutase activities and concentrations and myeloperoxidase activities in leukocytes from patients with diabetes mellitus. *J Diabetes Complications* 13: 264–270, 1999.
37. **VanTeeffelen JW, Constantinescu AA, Vink H, Spaan JA.** Hypercholesterolemia impairs reactive hyperemic vasodilation of 2A but not 3A arterioles in mouse cremaster muscle. *Am J Physiol Heart Circ Physiol* 289: H447–H454, 2005.
38. **Wolin MS, Rodenburg JM, Messina EJ, Kaley G.** Similarities in the pharmacological modulation of reactive hyperemia and vasodilation to hydrogen peroxide in rat skeletal muscle arterioles: effects of probes for endothelium-derived mediators. *J Pharmacol Exp Ther* 253: 508–512, 1990.
39. **Wu R, Millette E, Wu L, de Champlain J.** Enhanced superoxide anion formation in vascular tissues from spontaneously hypertensive and desoxycorticosterone acetate-salt hypertensive rats. *J Hypertens* 19: 741–748, 2001.
40. **Yada T, Hiramatsu O, Kimura A, Goto M, Ogasawara Y, Tsujioka K, Yamamori S, Ohno K, Hosaka H, Kajiya F.** In vivo observation of subendocardial microvessels of the beating porcine heart using a needle-probe videomicroscope with a CCD camera. *Circ Res* 72: 939–946, 1993.
41. **Yada T, Hiramatsu O, Kimura A, Tachibana H, Chiba Y, Lu S, Goto M, Ogasawara Y, Tsujioka K, Kajiya F.** Direct in vivo observation of subendocardial arteriolar response during reactive hyperemia. *Circ Res* 77: 622–631, 1995.

41a. **Yada T, Shimokawa H, Hiramatsu O, Haruna Y, Morita Y, Kashihara N, Shinozaki Y, Mori H, Goto M, Ogasawara Y, Kajiya F.** Cardioprotective role of endogenous hydrogen peroxide during ischemia-reperfusion injury in canine coronary microcirculation in vivo. *Am J Physiol Heart Circ Physiol* 291: H1138–H1146, 2006.

42. **Yada T, Shimokawa H, Hiramatsu O, Kajita T, Shigeto F, Goto M, Ogasawara Y, Kajiya F.** Hydrogen peroxide, an endogenous endothelium-derived hyperpolarizing factor, plays an important role in coronary autoregulation in vivo. *Circulation* 107: 1040–1045, 2003.
44. **Yada T, Shimokawa H, Hiramatsu O, Shinozaki Y, Mori H, Goto M, Ogasawara Y, Kajiya F.** Important role of endogenous hydrogen peroxide in pacing-induced metabolic coronary vasodilatation in dogs in vivo. *J Am Coll Cardiol* 50: 1272–1278, 2007.
45. **Zhang DX, Gutterman DD.** Mitochondrial reactive oxygen species-mediated signaling in endothelial cells. *Am J Physiol Heart Circ Physiol* 292: H2023–H2031, 2007.

Acta Physiol 2007, 191, 275–284

Characterization of ouabain-induced noradrenaline and acetylcholine release from *in situ* cardiac autonomic nerve endings

T. Yamazaki,[1] T. Akiyama,[1] H. Kitagawa,[1] F. Komaki,[1] H. Mori,[1] T. Kawada,[2] K. Sunagawa[2] and M. Sugimachi[2]

1 Department of Cardiac Physiology, National Cardiovascular Center Research Institute, Suita, Osaka, Japan

2 Department of Cardiovascular Dynamics, National Cardiovascular Center Research Institute, Suita, Osaka, Japan

Received 11 January 2007, revision requested 28 March 2007, revision received 29 May 2007, accepted 30 June 2007
Correspondence: T. Yamazaki, Department of Cardiac Physiology, National Cardiovascular Center Research Institute, 5-7-1 Fujishirodai, Suita, Osaka 565, Japan. E-mail: yamazaki@ri.ncvc.go.jp

Abstract

Aim: Although ouabain modulates autonomic nerve ending function, it is uncertain whether ouabain-induced releasing mechanism differs between *in vivo* sympathetic and parasympathetic nerve endings. Using cardiac dialysis, we examined how ouabain induces neurotransmitter release from autonomic nerve ending.

Methods: Dialysis probe was implanted in left ventricle, and dialysate noradrenaline (NA) or acetylcholine (ACh) levels in the anaesthetized cats were measured as indices of neurotransmitter release from post-ganglionic autonomic nerve endings.

Results: Locally applied ouabain (100 μM) increased in dialysate NA or ACh levels. The ouabain-induced increases in NA levels remained unaffected by cardiac sympathetic denervation and tetrodotoxin (Na^+ channel blocker, TTX), but the ouabain-induced increases in ACh levels were attenuated by TTX. The ouabain-induced increases in NA levels were suppressed by pretreatment with desipramine (NA transport blocker) and augmented by reserpine (vesicle NA transport blocker). In contrast, the ouabain-induced increases in ACh levels remained unaffected by pretreatment with hemicholinium-3 (choline transport blocker) but suppressed by vesamicol (vesicle ACh transport blocker). The ouabain-induced increases in NA levels were suppressed by pretreatment with ω-conotoxin GVIA (N-type Ca^{2+} channel blocker), verapamil (L-type Ca^{2+} channel blocker) and TMB-8 (intracellular Ca^{2+} antagonist). The ouabain-induced increases in ACh levels were suppressed by pretreatment with ω-conotoxin MVIIC (P/Q-type Ca^{2+} channel blocker), and TMB-8.

Conclusions: Ouabain-induced NA release is attributable to the mechanisms of regional exocytosis and/or carrier-mediated outward transport of NA, from stored NA vesicle and/or axoplasma, respectively, while the ouabain-induced ACh release is attributable to the mechanism of exocytosis, which is triggered by regional depolarization. At both sympathetic and parasympathetic nerve endings, the regional exocytosis is because of opening of calcium channels and intracellular calcium mobilization.

Keywords acetylcholine, Ca^{2+} channels, cat, microdialysis, Na^+,K^+-ATPase, noradrenaline.

 doi: 10.1111/j.1748-1716.2007.01749.x